Quantifying the Potential of Electric Vehicles to Provide Electric Grid Benefits in the MISO Area

Final report to the Midcontinent Independent System Operator Inc.

Jeffery Greenblatt,[1,2] Cong Zhang,[1] Samveg Saxena (PI)[1]
[1]Lawrence Berkeley National Laboratory, Berkeley, CA
[2]Emerging Futures, LLC, Berkeley, CA

Table of Contents

Executive Summary

Electric vehicles (EVs) have seen explosive growth worldwide since 2010, recently surpassing 1 million vehicles in the U.S. and 4 million globally in late 2018. Even in the Midcontinent Independent System Operator (MISO) region, where EV sales have historically been about 34% of the U.S. average, vehicles are expected to reach between 1.6 and 36 million by 2039, as compared to ~50,000 EVs sold between 2011 and 2018. See Fig. ES-1.

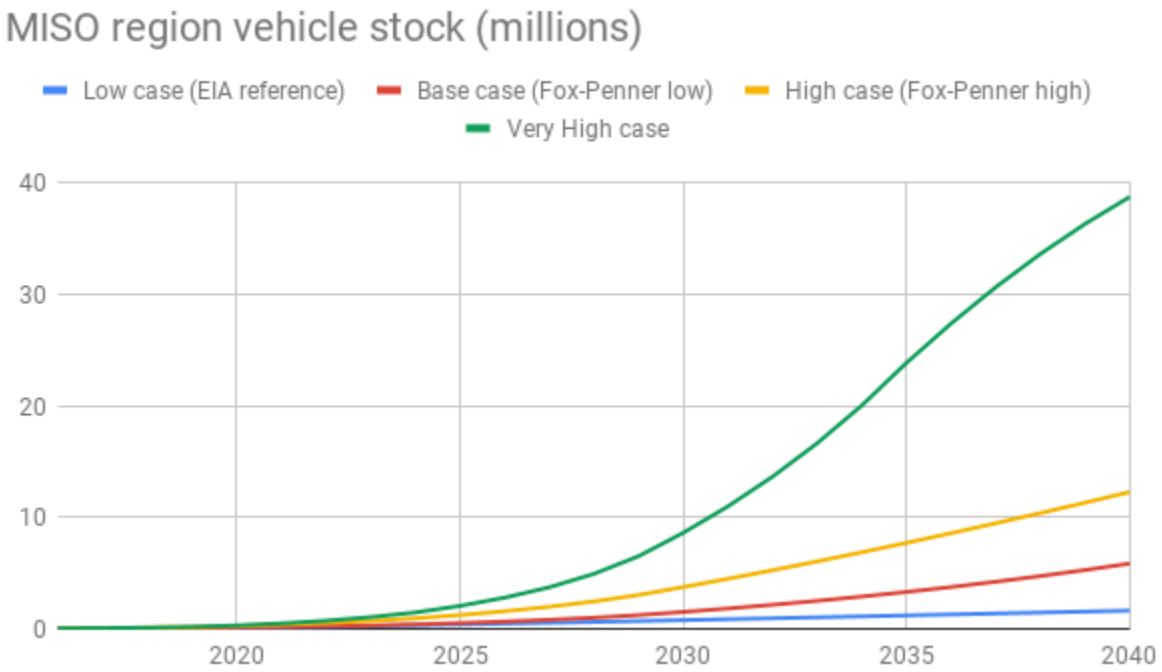

Fig. ES-1. Projected EV stocks (cumulative sales minus retirements) by scenario in the MISO region.

Increasing renewable generation on the MISO grid—to between 22% and 39% of projected future load in 2038, depending on scenario—will exacerbate daily load troughs and morning/evening ramps that will require new grid resources to mitigate. Fig. ES-2 illustrates these challenges. Uncontrolled EV charging (the type of charging available today) will exacerbate daily peaks, contributing to these challenges. Fortunately, controlled EV charging can mitigate both their own charging problems and the challenges of renewables integration. A number of pilot studies in the U.S. and around the world are currently exploring the value of controlled charging to electricity grids.

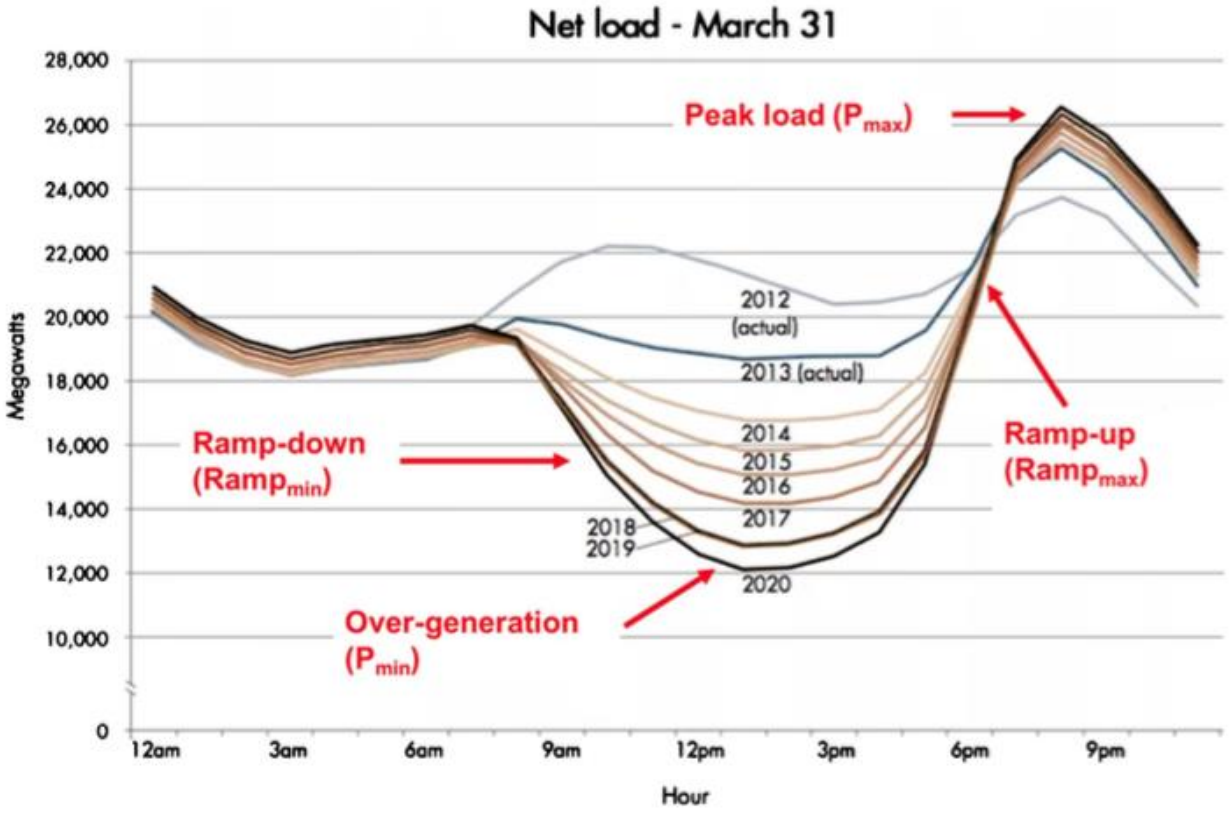

Fig. ES-2. Illustration of the net load "Duck Curve," highlighting the four regions of concern to grid operators.

This study was undertaken in order to quantify the effects of adding large numbers of EVs to the MISO grid over the next 20 years (2019-2039). For each of four EV penetration scenarios, we explored two renewable generation scenarios whose 2039 renewable generation varied by approximately a factor of two. EVs were allowed to charge in an uncontrolled manner in one scenario, and we explored four types of controlled charging optimizations, consisting of unidirectional ("V1G") and bidirectional ("V2G") charging operating under two complementary optimization schemes: peak shaving/valley filling ("peak-valley") control, and ramp mitigation ("ramp") control. We included a few scenarios where the charging infrastructure assumptions were revised. We also explored optimizations within two local resource zones (LRZs) for the high-renewables scenario: LRZ 1 (consisting primarily of Minnesota, with parts of North Dakota, South Dakota, Wisconsin and Montana) and LRZ 7 (Michigan). These two LRZs were chosen to explore differences in the ratio of renewable generation to the number of EVs.

High-level results indicate that without controlled charging, EVs tend to add load during peak periods of the day, exacerbating generation peaks and up- and down-ramps. In the extreme case of the Very High EV penetration scenario near the end of the simulation period (e.g., in 2038), EV charging dominates loads throughout the day and adds >40,000 MW to peak loads. Fortunately, we also find that all four types of controlled charging optimizations can have an equally profound effect on changing MISO's net load to make it more manageable.

While V1G can be effective at keeping peak daily loads close to what they would be without EVs even at small EV penetrations, by shifting load to other times of day (primarily nighttime load valleys), V2G is able to have a much stronger impact on load shapes for the same numbers of EVs because of its ability to return power to the grid, reducing loads below what they would be without EVS. As a result, V2G optimizations are able to greatly reduce peak loads, and for sufficiently large numbers of EVs, transform daily load variations into profiles that vary slowly over multiple days ("multi-day optimization"). In the extreme case of the Very High EV penetration scenario in 2038, both peak-valley and ramp V2G control optimizations can produce nearly flat loads over the week. But for smaller numbers of EVs, transformations approaching this result are also obtained.

Fig. ES-3 provides an overview of the effect of V1G and V2G controlled charging for the Base case of ~2.5 million EVs in 2032. Note the large differences in net load shape among the V1G control algorithms (green and cyan curves) versus V2G peak-valley control (magenta) and V2G ramp control (red). In the latter case, the optimization has become multi-day, where the algorithm is able to adjust the initial net load shape across multiple days.

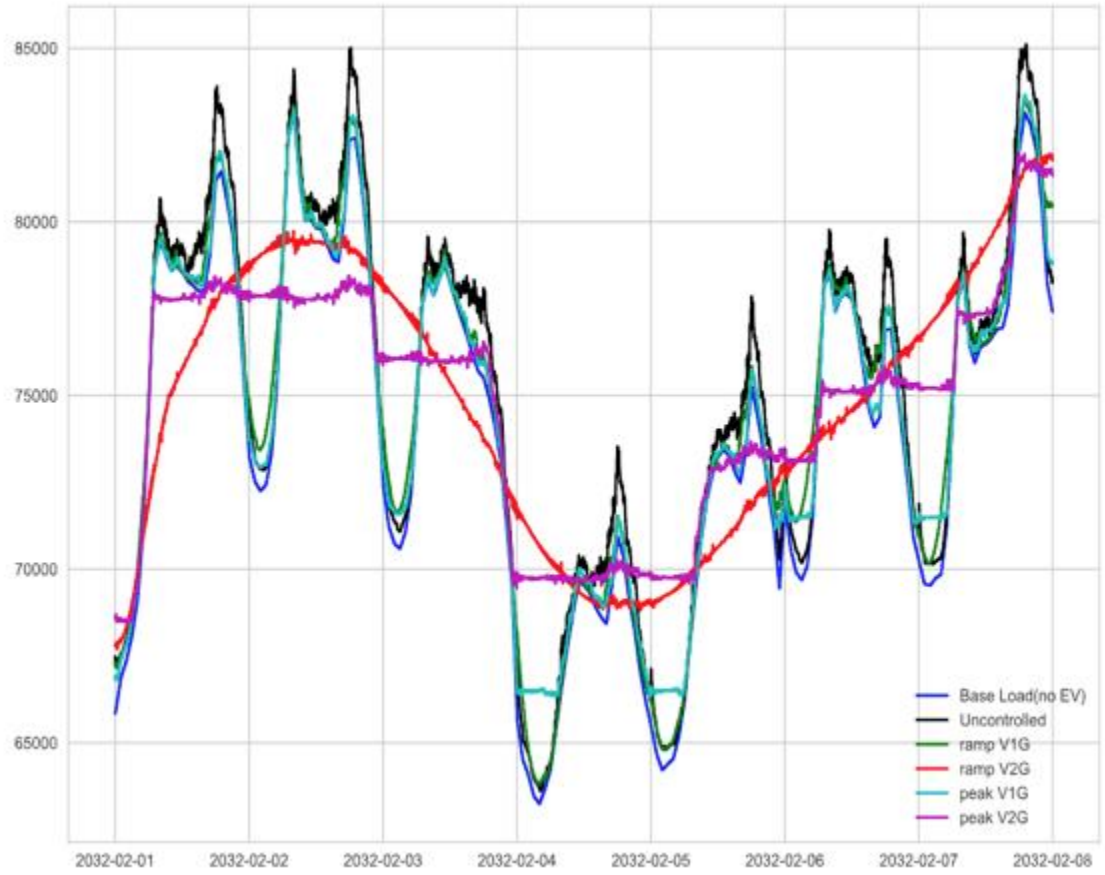

Fig. ES-3. Controlled charging effects for the Base EV penetration scenario, February 2032. Y-axis units are MW.

The effect of increasing renewable penetrations on the MISO grid in the absence of EVs is to reduce net loads and exacerbate differences between daily peaks and valleys. These changes lead to somewhat diminished effectiveness of controlled charging on modifying net loads, though the effects are fairly subtle; the conclusion is that while differences in load shape will occur, the controlled charging algorithms are nearly as effective at high renewable penetrations as at lower ones. Critically, controlled charging is able to greatly ameliorate the differences between peaks and valleys caused by renewable generation, producing a net load that is much easier for MISO to manage.

The impact of revising the charging infrastructure assumptions (somewhat less home charging, significantly less workplace charging, and a small increase in the amount of public charging) to better reflect expected future implementation results in very similar V1G charging profiles, but larger day-to-day load excursions among V2G charging profiles, indicating less load shifting capacity overall. However, the load-shifting capacity is still very significant at a sufficiently high EV penetration level.

Our exploration of local resource zones indicates that when renewables are sufficiently high as for LRZ 1, net loads can fall below zero, resulting in either an export of excess renewable generation to other LRZs, or renewables curtailment. The effect of the controlled charging algorithms on load shapes is unaffected by the absolute net load level, even when it is negative, and closely resembles results for MISO as a whole. Controlled charging (both V1G and V2G) is able to reduce these negative valleys, and with sufficient numbers of EVs can eliminate them altogether, obviating the need for either export of excess renewable generation or curtailment.

Fig. ES-4 illustrates these points, showing how a net load profile where load becomes negative at several points throughout the week is converted to net positive load at all times with controlled charging (both V1G and V2G). For the case where there are more EVs and less renewable generation (e.g., LRZ 7, not shown here), negative net load does not occur, and the controlled charging algorithms are more effective at shifting loads than for MISO as a whole, due to locally higher numbers of EVs per unit of load.

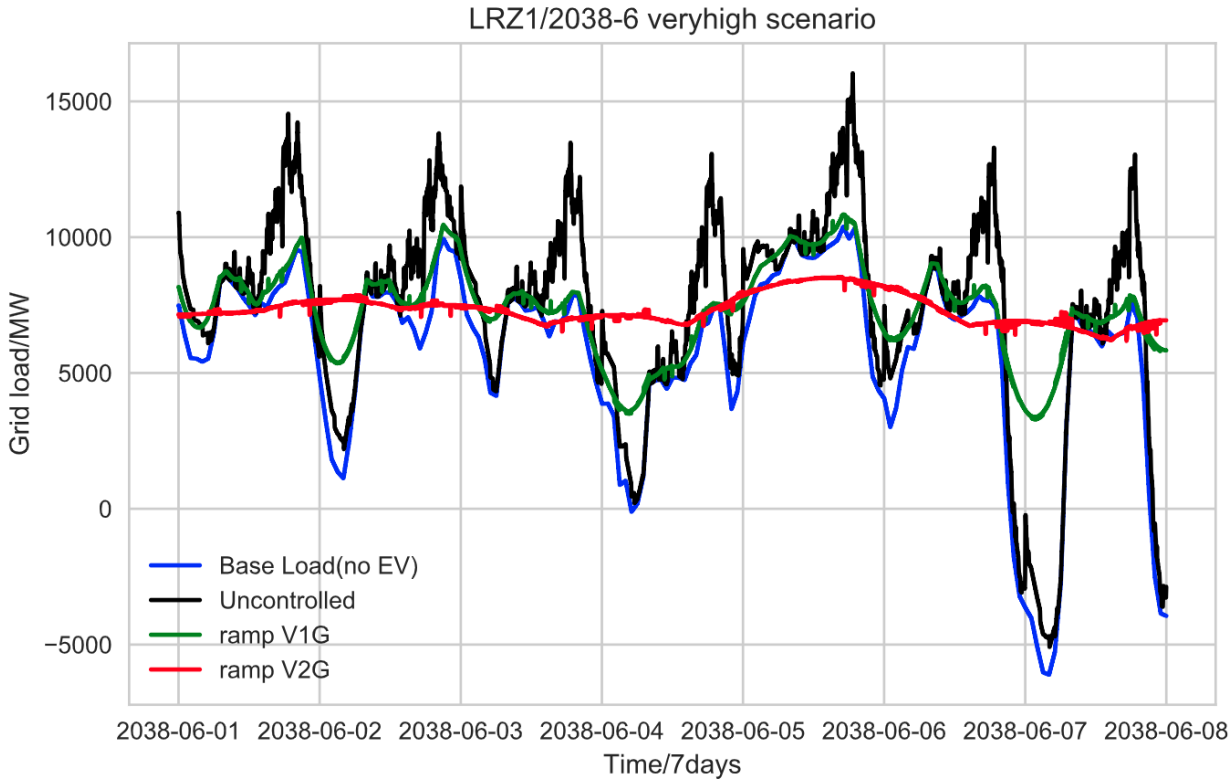

Fig. ES-4. Very High EV penetration scenario for LRZ 1 in June 2038.

In conclusion, we have demonstrated that controlled charging can be an effective tool at mitigating both the peak exacerbation effect of large numbers of EVs, as well as increased peak-valley differences (and potentially negative net loads) of high amounts of renewable generation. Whether V1G or V2G, and peak-valley or ramp control, is optimal for MISO will depend on many future assumptions and conditions, and likely a blend of these and other control algorithms will be most suitable to the particular future needs of the MISO grid. However, because of long lead times in deploying and integrating controlled charging equipment with other grid service products, the time is now to start planning for large numbers of EVs on the MISO grid with controlled charging to minimize grid impacts and maximize grid utility.

1. Introduction

1.1. Electric vehicle trends

For the purposes of this report, electric vehicles (EVs) are defined as any light-duty passenger vehicle that has an electric plug to recharge its onboard battery, and can be operated entirely on electricity if desired. Thus, both "pure" battery electric vehicles (BEVs) and plug-in hybrid electric vehicles (PHEVs), which can also run on gasoline or diesel fuel, are included as EVs. Sometimes hydrogen-powered vehicles are referred to as fuel cell electric vehicles (FCEVs) and included as part of EV sales, but as these vehicles generally do not have an electric plug and cannot be powered by electricity, we exclude them in this context.

EV sales have been growing rapidly since 2010. Fig. 1 shows monthly sales in the U.S. and cumulative sales in both the U.S. and in California, a state that has historically contributed nearly 50% of U.S. sales. Cumulative U.S. sales surpassed 1 million vehicles, and 500,000 vehicles in California, in late 2018. Annual U.S. growth in sales was 75% in 2018, the highest annual growth rate since 2013.

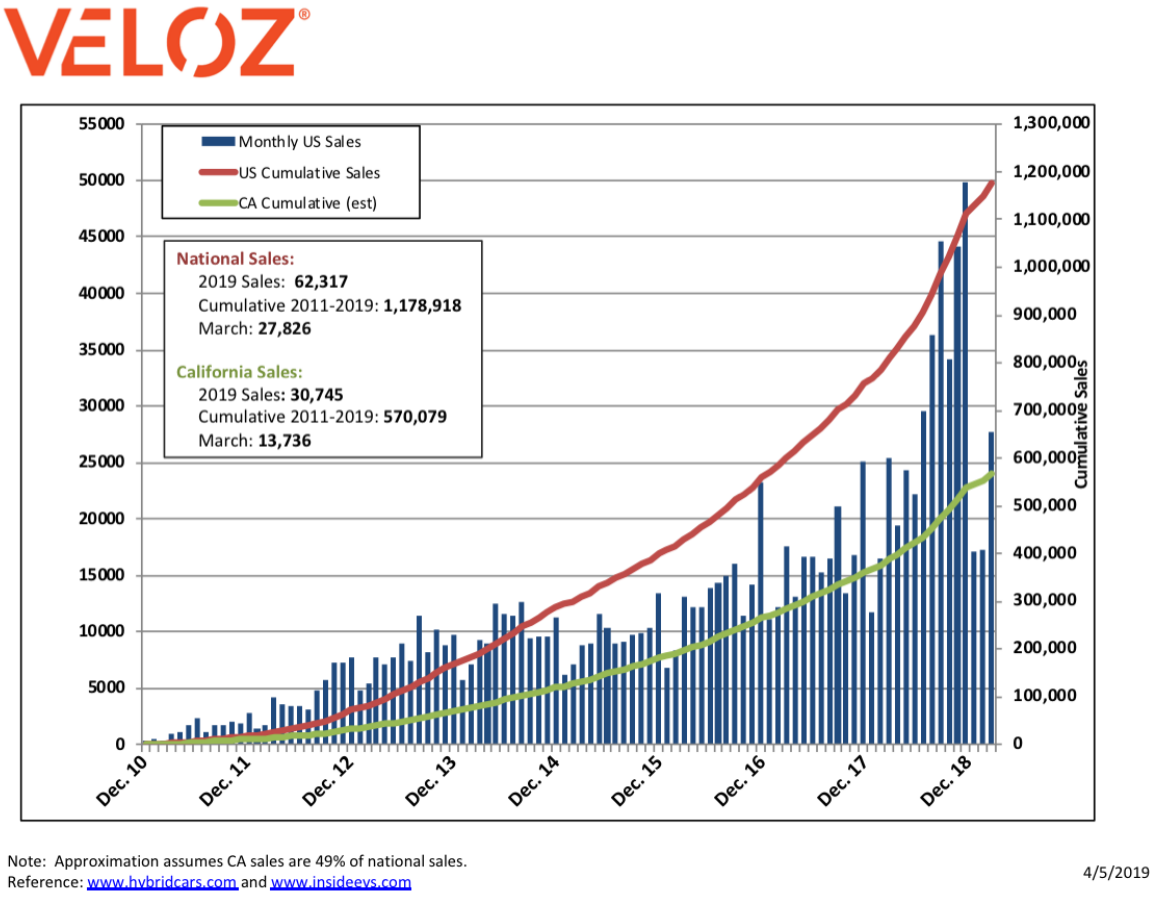

Fig. 1. Monthly U.S. and cumulative U.S. and California EV sales. Source: Veloz (2019), with minor modifications made for clarity.

Globally, sales have been even stronger, than in the U.S., with cumulative sales passing 4 million vehicles in Q3 2018, with 5 million cumulative sales forecast by 1Q 2019. See Fig. 2.

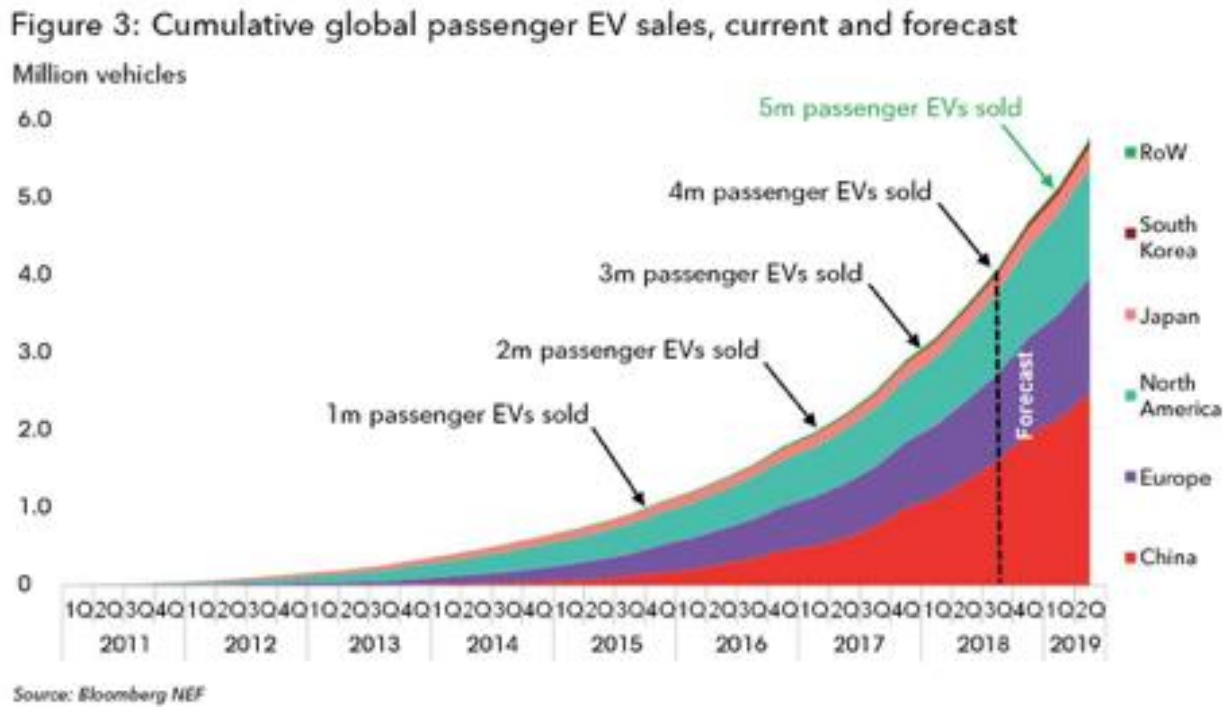

Fig. 2. Cumulative global passenger EV sales. Source: Bloomberg (2018a).

Sales in China in particular were 175% higher than January of last year, representing 4.8% of market share. Analysts estimate that sales in 2019 may surpass 2 million, compared to 1.1 million in 2018 (Kane, 2019).

Bloomberg New Energy Finance (Bloomberg, 2018b) forecasts that global EV sales will increase to 11 million in 2025 and 30 million in 2030, with sales in China accounting for almost 50% of the global market in 2025 and 39% in 2030. By 2040, Bloomberg forecasts there will be 60 million EVs sold annually, representing 55% of new vehicle sales, adding up to 559 million EVs on the road and 33% of the global car fleet (Bloomberg, 2018b).

In terms of number of models, there are 44 EV models currently for sale in the U.S. (EVAdoption, 2019). Globally, the number of available models was set to increase from 155 at the end of 2017 to 289 by 2022, according to Bloomberg (2018b). Several companies, including VW, Daimler, Nissan, Volvo and Chang'an have made plans to electrify their vehicles over the next 10 years (Bloomberg, 2018b).

Battery costs, the single most expensive component in an EV that accounts for most of the cost difference with conventional combustion vehicles, has been falling from $1,000/kWh in 2010 to ~$200/kWh in 2017, and is projected to fall below $100/kWh in 2025 (Bloomberg, 2018b). See Fig. 3. In 2017, Bloomberg forecast that EVs will reach upfront cost parity with combustion vehicles on an unsubsidized basis starting in 2026, and every year since this crossover point

forecast has been moving up in time; its latest 2019 analysis suggests that it will now occur in 2022 (Bullard, 2019).

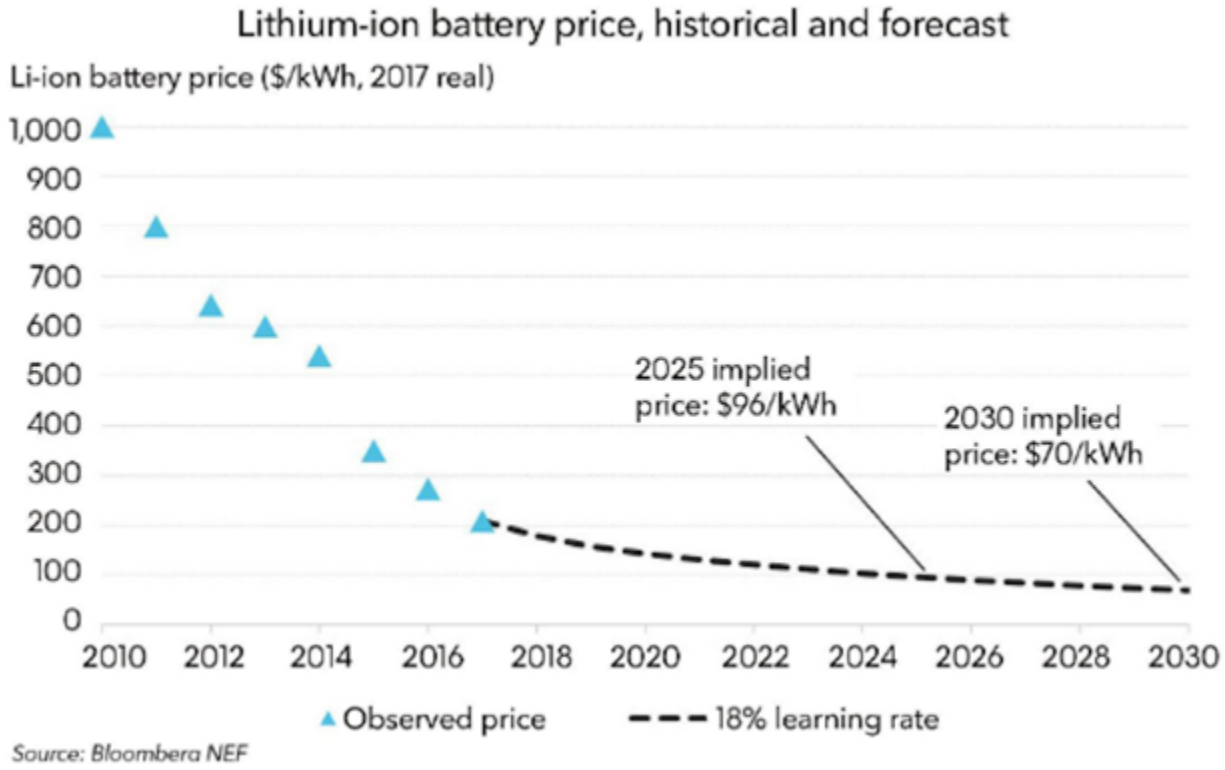

Fig. 3: Lithium-ion battery price history and forecast. Source: Bloomberg (2018b).

Eleven countries including China, India, France and the United Kingdom, representing nearly 3 billion people or 39% of global population have announced phase-outs of internal combustion engine vehicles between 2021 and 2040, and an additional 20 cities and territories have announced similar bans, at least for diesel vehicles (Wikipedia, 2019). Such phase-outs will likely further accelerate the adoption of EV sales.

1.2. Electric grid trends

In the U.S., the share of electricity provided by non-greenhouse gas emitting sources has been steadily growing, and now stands at 1,487 billion kilowatt-hours (terawatt-hours or TWh) annually, or 38% of total electricity generation. Of this, 54% is nuclear power and 19% is conventional hydropower, neither of which is considered “renewable.” Renewables currently provide 10.5% of total electricity generation, with wind power reaching 289 TWh/yr or 7.3% of electricity generation in 2019, surpassing hydropower for the first time (EIA, 2019). Today, much of that wind power is concentrated in the Plains States that fall within MISO’s footprint, with the following four states each generating more than 60% of its electricity from renewables: Iowa (92%), Minnesota (66%), Nebraska (61%) and South Dakota (94%) (DOE, no date).

Because of an expected reduction in overall nuclear capacity, renewables will surpass nuclear generation in 2021, and their continued growth will put them on track to reach 15% of electricity generation in the late 2020s, dominated by wind power (~60%) and solar photovoltaics (PV) (~30%) (EIA, 2019). Twenty-nine states, including Illinois, Iowa, Michigan, Minnesota, Missouri, Texas and Wisconsin within the MISO footprint, have Renewable Portfolio Standard (RPS) policies that require a certain fraction of energy to be supplied by renewables by certain target years, and an additional eight states have voluntary renewable energy targets. Most states target between 10% and 45% renewable electricity generation, whereas seven states—California, Hawaii, Massachusetts, New Jersey, New York, Oregon, and Vermont—plus Washington, D.C. have requirements of 50% or greater (National Conference of State Legislatures, 2019).

Globally, renewable generation is skyrocketing, with total installed capacities of renewables in 2017 at 1,081 GW, dominated by wind power (50%) and solar PV (37%). Hydropower provides an additional 1,114 GW of capacity. Most generation occurs outside the U.S., and China now dominates in both wind and solar PV, contributing 31% of total renewable capacity, roughly double that of the U.S. Nearly 90 countries have RPS or similar renewable energy targets that are as if not more aggressive than those of many U.S. states (REN21, 2018).

With the expected increases in renewable generation come concerns about balancing increasingly variable supply with demand, and much has been written on this subject. The general conclusion is that with more renewables comes a greater need for flexible loads, if the reliance on fossil-based dispatchable generation technologies is to be avoided. Such flexible loads include traditional demand response opportunities associated with large electricity-consuming devices in the commercial and industrial sectors, as well as smaller, more distributed loads such as electric heat pumps and electric vehicles in the commercial and residential buildings sectors (Greenblatt, 2017).

1.3. Controlled charging

Unlike most rechargeable devices that begin charging as soon as they are plugged in, and stop charging as soon as the battery is full, controlled charging provides flexibility in the time evolution of vehicle charging, with potential benefits to both the electric grid (in terms of reduced operational costs through managing total loads) and the vehicle user (in terms of reduced charging costs).

In terms of charging speeds, level 1 (L1) charging uses the existing wall outlet (120 V) to provide up to 1.4 kW of power. Level 2 (L2) uses a specialized plug that operates at higher voltage (208-240 V) and current to deliver up to 20 kW of power. Level 3 (L3), also known as DC Fast Charging (DCFC), uses even higher direct-current voltage (480 V) to provide 50 kW or more power. Fig. 4 shows these three levels along with some additional information.

Fig. 4. Comparison of charging speed standards used with EVs. Source: Authors.

There are basically two types of controlled charging: unidirectional ("V1G") and bidirectional ("V2G"). V1G allows the flow of power from the grid to the vehicle to vary over the course of a charging session. This power flow can be dictated by a simple timer, a price signal from the grid operator, or more complex rules of when to charge or not charge according to certain grid conditions. V2G operates the same way, but power is also able to flow from the vehicle to the grid, helping alleviate grid stress particularly during peak power demands. As can be seen from Fig. 5, the dynamic power range of V2G is twice that of V1G for a specified charging level.

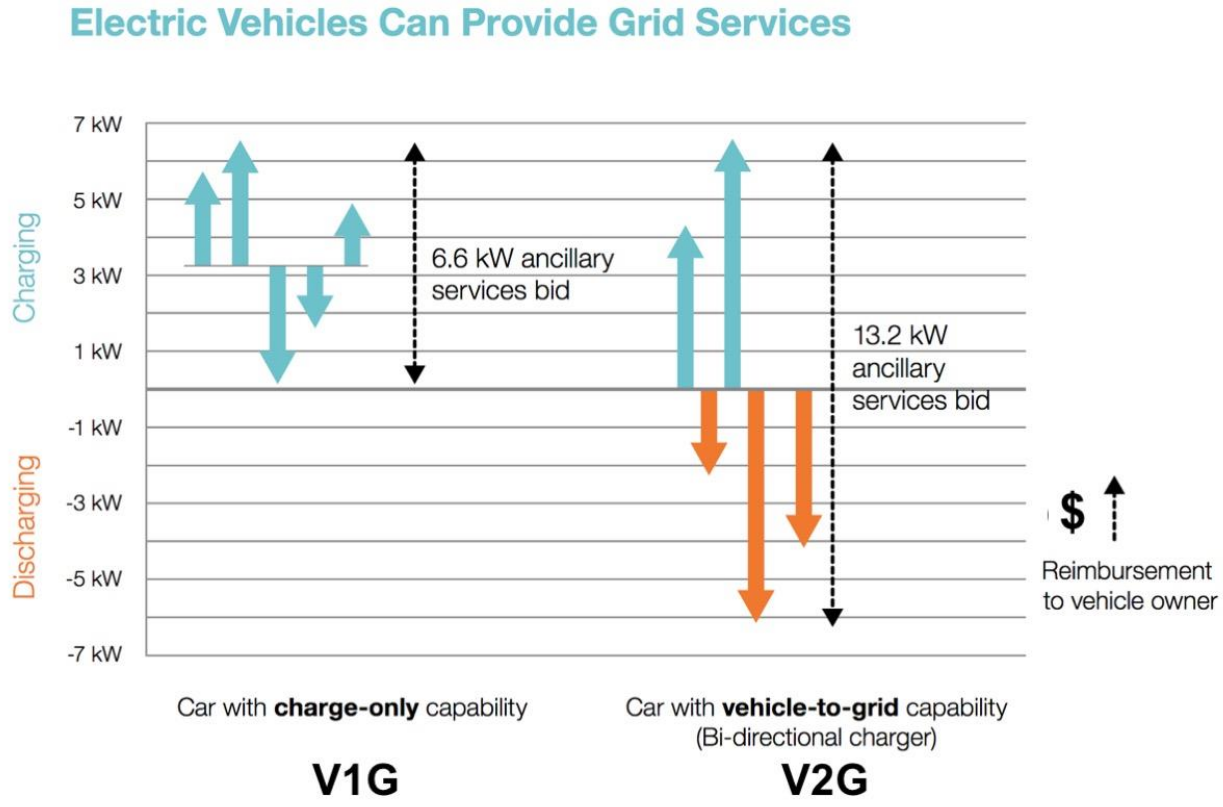

Fig. 5. Differences between V1G and V2G charging. Source: Newmotion (no date) with modifications made for clarity.

While neither V1G nor V2G is commercial yet, a number of controlled charging pilot studies have been conducted or are ongoing, some of which are summarized in Table 1.

Table 1. A sampling of controlled charging pilots

Location	Partner(s)	Type	Direction-ality	Status	Comments
Los Angeles, CA	Los Angeles Air Force Base, Berkeley Lab, Southern California Edison, California ISO (CAISO), California Energy Commission, Kisensum, LLC	Ancillary services (frequency regulation) market, load-shifting in buildings, demand response	V2G, vehicle-to-buildings (V2B)	Completed (2016-2017)	29 EVs using automatic generation control from CAISO as signal input[a,b]
Los Angeles, CA	Los Angeles Air Force Base, Berkeley Lab	Study	V2G, V2B	Ongoing	Second-life batteries and accelerated degradation[a]
Alameda County, CA	Alameda County, Berkeley Lab, Prospect Silicon Valley, ChargePoint, Kisensum, LLC	Peak-shaving peak demand management	V1G	Completed (2013-2018)	>40 fleet EVs using level 1 and level 2 charging. Innovative public interface to gather information on charge duration, spreading of recharging[a,c]
California	BMW, UC Berkeley	XBOS-V[d] building and smart vehicle control	V1G	Close to completion	Trying to find value proposition[a]
California	Nuvve, UC San Diego	Research	V2G	Ongoing	Have great field site, working on second-life batteries, microgrids[a]
California	ChargePoint, San Diego Gas & Electric	Direct customer interface with price signals	V1G	Completed	Mostly rewarding overnight charging[a]
California	eMotorWerks, CAISO	Proxy demand resource[e]	V1G	Announced (end of 2018)	Aggregation of 1000s of chargers and EVs[a]

		bidding into CAISO			
United States	Nissan	Unclear	V2B	Ongoing	Trying to commercialize V2G[a]
Colorado	eMotorWerks, Platte River Power Authority (CO)	Study	Pre-V1G	Announced (March 2019)	Study driver behavior of 250 smart chargers[f]
Nether-lands	ElaadNL, Greenflux, 12 partners from 6 EU countries	Unclear	V1G, V2G	Ongoing (2017-2020)	First smart charging project in Europe using communications open standards[g]
Amster-dam, Nether-lands	NewMotion, Alliander, Enervalis, Amsterdam Smart City	Unclear	V2G	Announced (March 2019)	Part of a Europe-wide project called City Zen[h]
United Kingdom	Smart Power Systems, Flextricity, Flexisolar, Turbo Power Systems	Unclear	V2G	Launched	Seeking commercial adopters for 6 sites, 150 V2G-capable EVs[i]
United Kingdom	EDF Energy, Nuvve	Market participation during peak energy use	V2G	Announced (October 2018)	1,500 chargers, EVs provide up to 15 MW storage[j]

Sources: [a]D. Black (pers. commun., 2019), [b]Black et al. (2017), [c]Black et al. (2019), [d]Lipman and Calloway (2017), [e]CAISO (2019), [f]Evarts (2019), [g]ElaadNL (2019), [h]FleetEurope (2019), [i]Smart Energy International (2019), [j]Business Wire (2018).

Of note is that in Japan, Nissan LEAFs used for V2G do not void the manufacturer's battery warranty, whereas this is still the case in the U.S. (D. Black, pers. commun., 2019).

1.4. Project objectives

The project objectives consisted of the following:

1. Provide defensible future projections of renewable generation and EV load profiles for 20 years into the future (2019-2039) in the MISO footprint, based on historical data, expected load growth trends, and renewable energy mandates.

2. Quantify the influence of EVs on the MISO grid for different assumptions about:
    a. Numbers of EVs deployed by year
    b. Charging infrastructure availability, types of uncontrolled vs. controlled charging
    c. Share of renewable energy generation
    d. Local resource zone (LRZ) conditions, e.g., numbers of EVs and renewable generation share
    e. How/when people charge their vehicles, e.g. home vs. work vs. public charging, L1 vs. L2 or faster charging
    f. Battery capacities (e.g., 24, 60 or 85 kWh)
    g. Type and fleet mix of EVs that are deployed (e.g. EVs and PHEVs)

3. Quantify the value of grid-integrated EVs by estimating the capital cost of EV charging and battery degradation due to controlled charging.

The project explored the impacts of items 2a through 2e. The last two items initially outlined in the proposal (2f and 2g) did not end up being pursued during this initial year of funding, but could become the focus of future work.

2. Analytical approach

2.1. Overview

Fig. 6 shows an overview of the analytical approach we took for the MISO project, which consists of the following components: net load forecasts, numbers of EVs, and travel itineraries individual vehicles in the MISO region are provided as inputs to the V2G-Sim modeling framework. This model consists of automatic drive-cycle generation, a vehicle powertrain model to simulate electricity consumption with realistic physics under variable driving conditions, a detailed battery model including simulating the effects of battery degradation, and a control algorithm to determine optimal EV charging according to a user-specified objective function. The resulting output is an optimized net load time series for every timestep in the simulation.

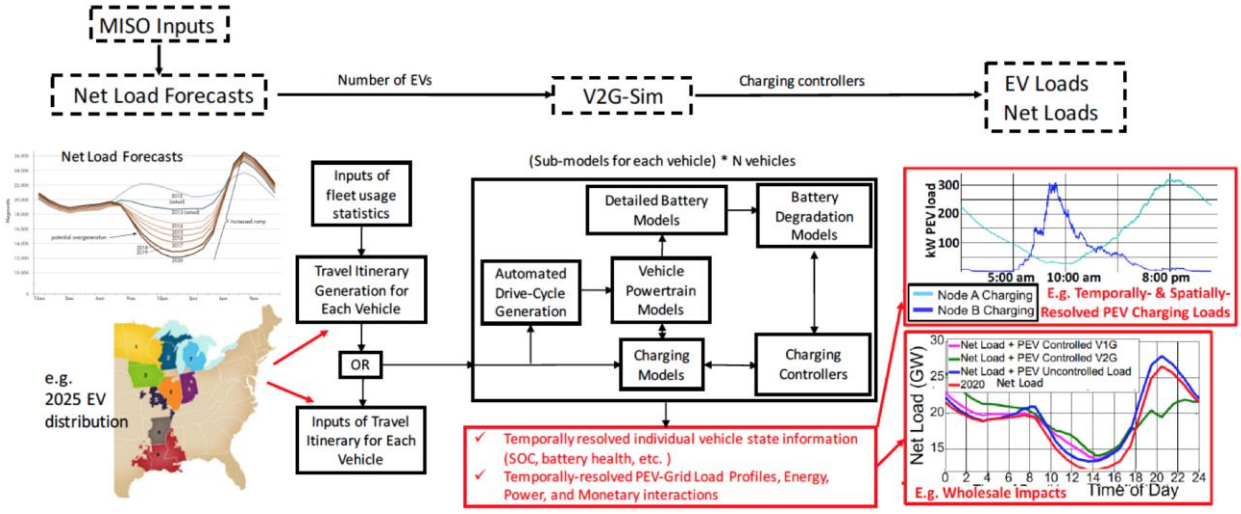

Fig. 6. Evaluating the influence of EVs on the future net load in the MISO area, using Berkeley Lab's *V2G-Sim model.* Source: Authors.

2.2. Vehicle-to-Grid Simulator model

The Vehicle-to-Grid Simulator (V2G-Sim) is a unique simulation tool developed using Lawrence Berkeley National Laboratory (Berkeley Lab)'s Laboratory Directed Research and Development (LDRD) funding. V2G-Sim quantifies second-by-second energy use for any number of different EVs while operating under varying driving conditions, or while connected to the grid and charging (or discharging).

With V2G-Sim, stakeholders in the electricity grid industry, automobile industry, and policy and regulatory sectors can predict how different vehicles will perform for different drivers, and how different vehicles will interact with the electricity grid. Grid operators and regulatory agencies can use V2G-Sim to forecast the amount of electricity demand for any time interval throughout the day. V2G-Sim will also help industry and policy stakeholders better understand how electric vehicles can integrate renewable energy sources, such as wind and solar, with the electricity grid by storing excess energy produced during windy or sunny periods, or providing energy back to the grid during peak demand periods. Fig. 7 summarizes how V2G-Sim can be applied by various stakeholders in vehicle- grid integration.

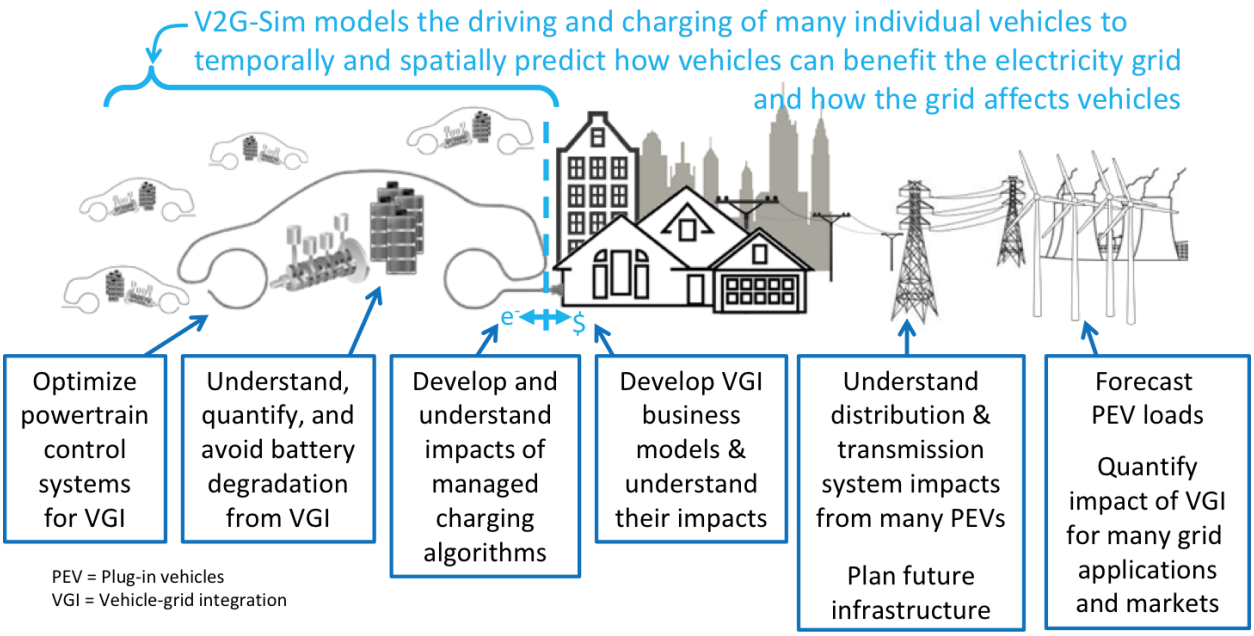

Fig. 7. Overview and example applications of V2G-Sim. Source: Authors.

2.3. Electric vehicle projections in the MISO region

Projections of EVs for the MISO region utilized three data components, illustrated in Fig. 8. The first data component was state-level EV sales data from Auto Alliance (2018) to provide total sales of battery-electric and plug-in hybrid EVs between 2011 and 2018 by U.S. state. City-level data from Slowik and Lutsey (2018) was also examined to corroborate the state-level data but was not used in the final analysis. The second component was state-level customer data provided by MISO, used to scale each state's EV sales data to sales within the MISO region. The third component was U.S.-wide EV sales forecasts from EIA (2018) and Fox-Penner et al. (2018), which itself was a compendium of several EV forecasts ranging from conservative to aggressive. These were used to scale the MISO-region sales fractions to overall U.S. sales. Finally, EV sales were converted to EV stock using a vehicle retirement function (EIA, 2018).

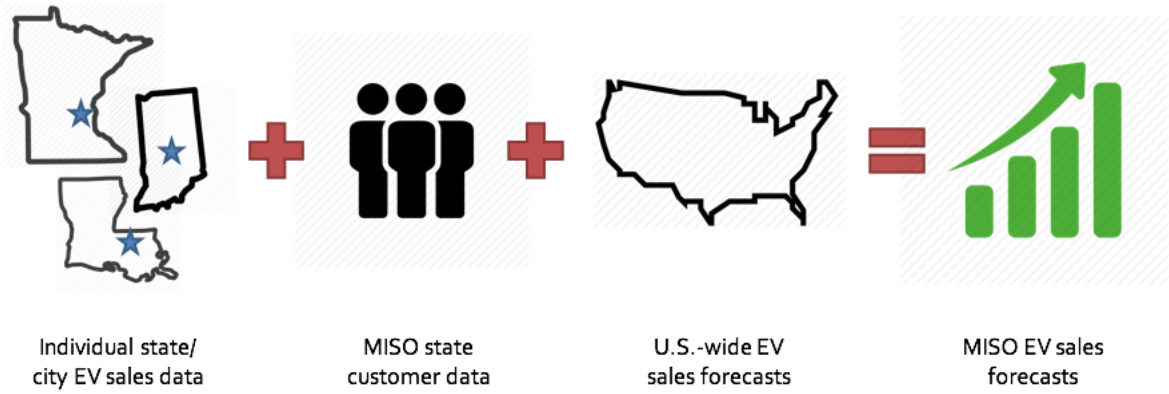

Fig. 8. Schematic of EV forecasting approach used for MISO. Source: Authors.

In examining Auto Alliance data from between January 2011 and August 2018, we plotted EV sales expressed as a fraction of overall U.S. sales for each year for the 15 states partially or wholly within the MISO region; see Fig. 9. Note that sales data for 2018 were projected for the full year, based on data through August. Subsequently, we obtained data for the entirety of 2018 and found that EV sales fractions were very similar to our earlier projections (Auto Alliance, 2019).

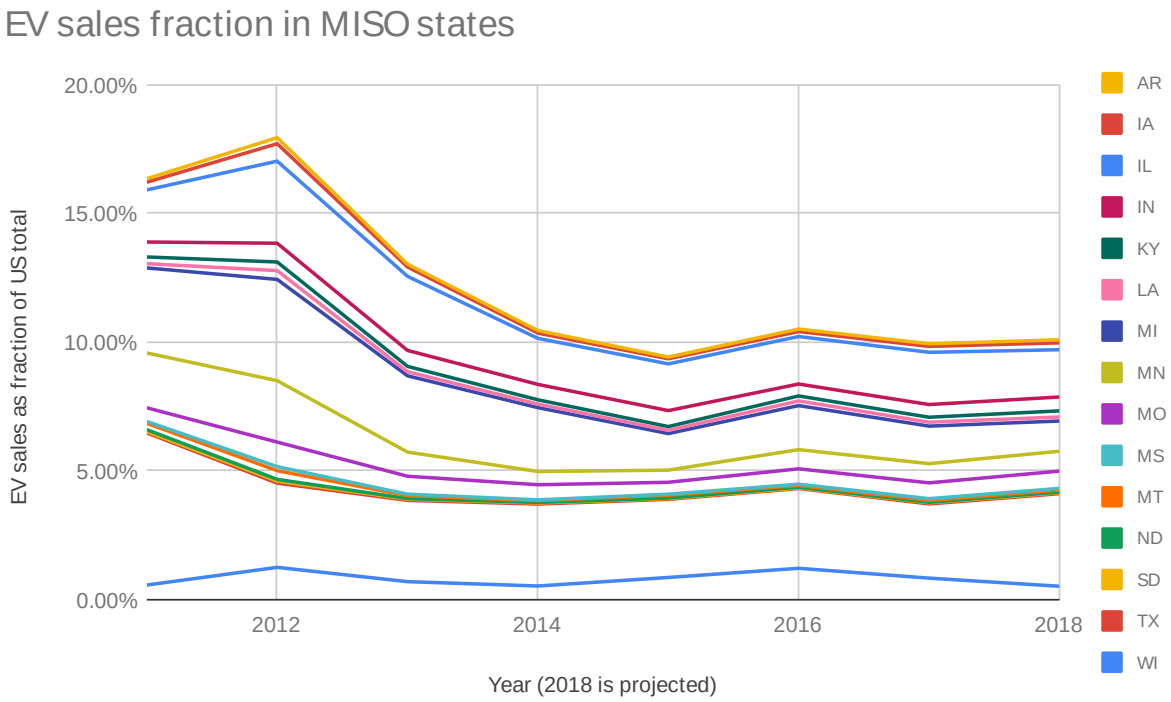

Fig. 9. EV sales fraction by year for MISO states. Source: Auto Alliance (2019), with analysis by authors.

We find that between 2014 and 2018, the fractions of sales within MISO states are fairly flat, indicating a lack of a strong positive or negative trend relative to the U.S. as a whole. Therefore, in projecting EV sales forward in time, the assumption that MISO states would continue to have a steady fraction of total U.S. sales appears to be reasonable. When weighting for the fraction of customers in each MISO state (see below), we found that the MISO region was responsible for an average of 4.71% of U.S. EV sales. Given that MISO's population share is 13.7% of the U.S., this represents sales that are 34% of the U.S. average.

We also examined EV sales from 2017 from Slowik and Lutsey (2018) for selected cities within and proximal to the MISO region, and found that average EV sales in MISO cities was 0.49%, as compared with 1.36% for the U.S. overall. This implies that sales within the MISO region constitute 36% of U.S. average sales, which is very consistent with our above estimate based on weighted state-level data.

We developed a total of four sets of scenario projections of future U.S. EV sales: Low, Base, High and Very High. The Low scenario was based on the Annual Energy Outlook 2018 Reference Case (EIA, 2018). The Low Case from Fox-Penner et al. (2018) was used as our Base scenario, and Fox-Penner et al.'s High Case was used as our High scenario. Finally, the Very High scenario was based on our High scenario, but with the fraction of MISO sales increasing toward California levels so that by 2039, 68% of vehicle stock in the MISO region are EVs. See Fig. 10.

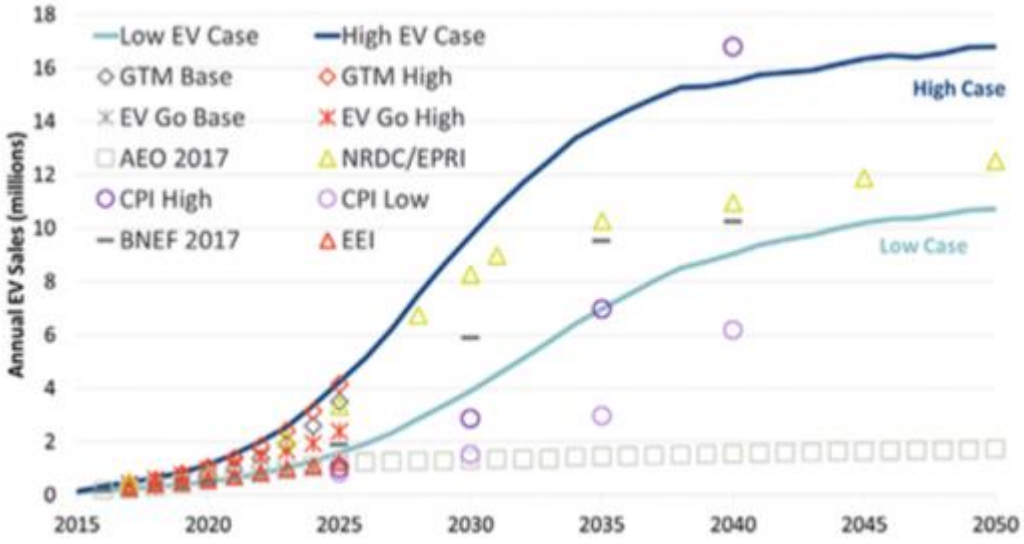

Fig. 2. U.S. EV sales projections.

Fig. 10. Various projections of U.S. EV sales through 2050. Source: Fox-Penner et al. (2018).

For all scenarios, vehicle stocks were calculated by integrating annual vehicle sales, minus a vehicle retirement fraction taken from EIA (2018). The results are shown in Fig. 11 and Table 2.

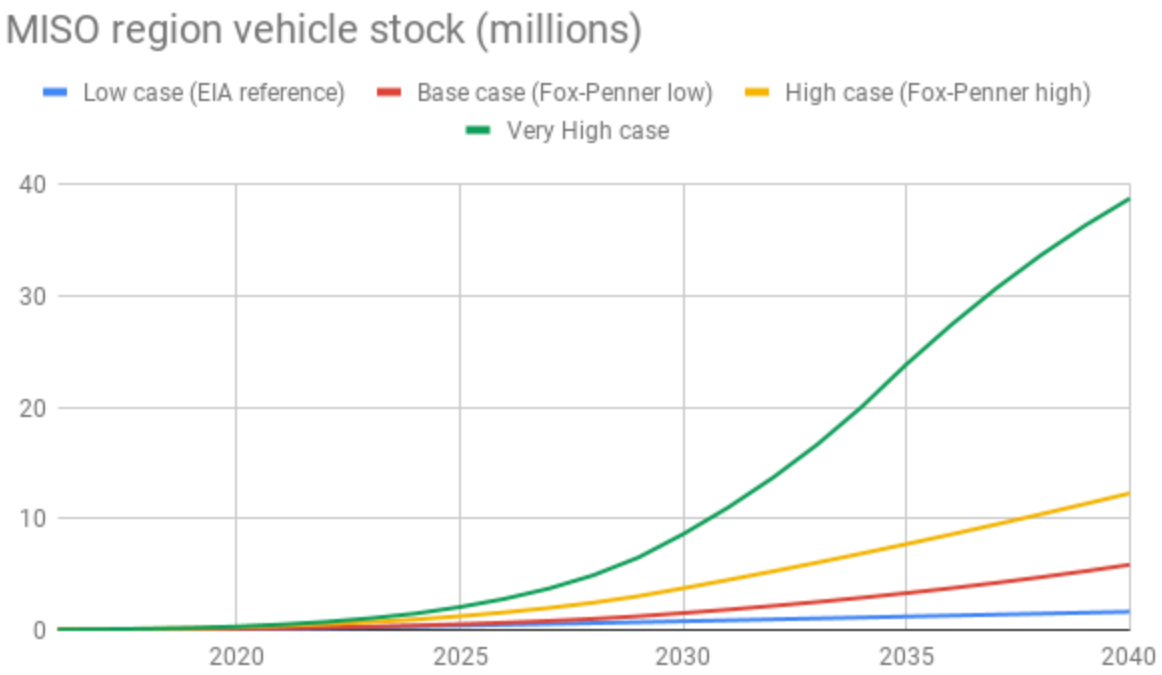

Fig. 11. Projected EV stocks by scenario in the MISO region. Sources: EIA (2018), Fox-Penner et al. (2018), and modeling by the authors.

Table 2. EV populations (millions) for the four EV penetration scenarios

	Year				
EV scenario	**2019**	**2024**	**2029**	**2034**	**2039**
Low	0.09	0.33	0.71	1.12	1.55
Base	0.09	0.40	1.24	2.90	5.28
High	0.16	0.95	3.04	6.87	11.32
Very High	0.19	1.48	6.52	20.05	36.34

Sources: EIA (2018), Fox-Penner et al. (2018), and modeling by the authors.

MISO provided us with data on the numbers of customers within each state in the MISO region that was also classified by LRZ. We used this data to scale the number of EV sales in each state to obtain EV sales by LRZ. Table 3 summarizes this data.

Table 3. Fraction of population in each state within each LRZ.

	LRZ									
State	**1**	**2**	**3**	**4**	**5**	**6**	**7**	**8**	**9**	**10**
AR	0.0%	0.0%	0.0%	0.0%	0.0%	0.0%	0.0%	76.5%	0.0%	0.0%
IA	0.0%	0.0%	90.4%	0.0%	0.0%	0.0%	0.0%	0.0%	0.0%	0.0%

IL	0.0%	0.0%	0.0%	22.1%	0.0%	0.0%	0.0%	0.0%	0.0%	0.0%
IN	0.0%	0.0%	0.0%	0.0%	0.0%	80.5%	0.0%	0.0%	0.0%	0.0%
KY	0.0%	0.0%	0.0%	0.0%	0.0%	0.0%	0.0%	0.0%	0.0%	0.0%
LA	0.0%	0.0%	0.0%	0.0%	0.0%	0.0%	0.0%	0.0%	89.6%	0.0%
MI	0.0%	1.5%	0.0%	0.0%	0.0%	0.0%	94.5%	0.0%	0.0%	0.0%
MN	95.4%	0.0%	0.0%	0.0%	0.0%	0.0%	0.0%	0.0%	0.0%	0.0%
MO	0.0%	0.0%	0.0%	0.0%	43.2%	0.0%	0.0%	0.0%	0.0%	0.0%
MS	0.0%	0.0%	0.0%	0.0%	0.0%	0.0%	0.0%	0.0%	0.0%	51.5%
MT	4.1%	0.0%	0.0%	0.0%	0.0%	0.0%	0.0%	0.0%	0.0%	0.0%
ND	71.7%	0.0%	0.0%	0.0%	0.0%	0.0%	0.0%	0.0%	0.0%	0.0%
SD	35.0%	0.0%	0.0%	0.0%	0.0%	0.0%	0.0%	0.0%	0.0%	0.0%
TX	0.0%	0.0%	0.0%	0.0%	0.0%	0.0%	0.0%	0.0%	4.9%	0.0%
WI	8.2%	91.6%	0.0%	0.0%	0.0%	0.0%	0.0%	0.0%	0.0%	0.0%

Source: MISO, Ventyx Velocity Suite, with analysis by the authors.

The data MISO provided also permitted us to make a more detailed estimate of MISO's share of the population in each state, which was later used to scale EV sales data by LRZ. Data and calculations are presented in Table 4.

Table 4. MISO customers within each state.

State	Retail customers in MISO region	Total retail customers	% in MISO	State population in 2017	Population in MISO region
AR	1,230,046	1,607,632	76.51%	3,004,319	2,298,692
IA	1,463,417	1,619,417	90.37%	3,145,698	2,842,670
IL	1,774,918	8,025,185	22.12%	12,801,518	2,831,292
IN	2,578,751	3,202,016	80.54%	6,666,801	5,369,123
KY	0	2,282,467	0.00%	4,453,929	0
LA	2,134,159	2,382,878	89.56%	4,684,382	4,195,438
MI	4,700,831	4,896,776	96.00%	9,962,203	9,563,564
MN	2,576,830	2,701,482	95.39%	5,576,383	5,319,077
MO	1,364,352	3,160,952	43.16%	6,113,185	2,638,615
MS	788,505	1,529,869	51.54%	2,983,978	1,537,963
MT	25,721	620,368	4.15%	1,050,326	43,547
ND	331,943	462,854	71.72%	755,389	541,739

SD	164,897	471,719	34.96%	869,627	303,992
TX	604,687	12,413,394	4.87%	28,299,599	1,378,543
WI	3,030,764	3,037,229	99.79%	5,795,359	5,783,023
Totals	22,769,821	48,414,238	47.03%	96,162,694	45,226,517

Source: MISO and World Population Review (no date).

2.4. Controlled charging algorithm implementation

Net electricity load is defined as the total base load (e.g., without EVs) minus renewable energy generation. As the amount of renewables on the grid increases, the daily net load shape changes, and takes on a form that to many resembles the profile of a duck, hence the term "Duck Curve"; see Fig. 12.

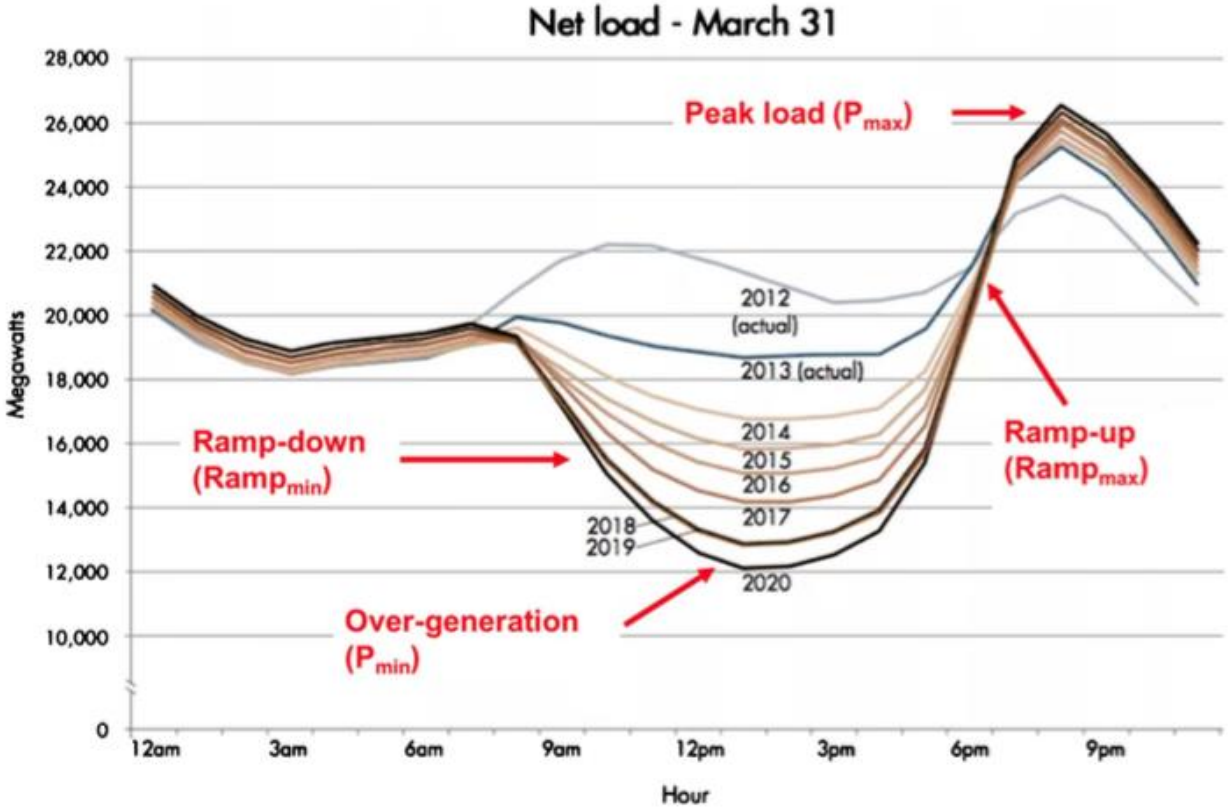

Fig. 12. Illustration of the net load "Duck Curve," highlighting the four regions of concern to grid operators. Source: Coignard et al. (2018).

The following four parameters depicted in Fig. 12 highlight regions of concern for grid operators, both in California and potentially elsewhere such as in MISO:

> P_{min}: Net load valley, which happens when load is low and renewable generation (mainly due to solar PV) is at a maximum. This may require either daily reductions in the output from large baseload generating stations, or curtailment of renewable generation.

P_{max}: Net load peak, which happens when load peaks for the day but there is little output from renewable generation.

$Ramp_{min}$: Sharp down-ramps, which happen when renewable output is rapidly increasing.

$Ramp_{max}$: Substantial up-ramps, which happen when load is increasing at the same time that renewable rapidly bringing generation is decreasing. This will require additional generation resources online and rapidly ramping up online resources (a technically difficult and potentially expensive challenge to be faced daily).

The purpose of implementing controlled charging is to address one or more of these regions of concern in the Duck Curve. In simulating controlled charging, we define three distinct ways that vehicles can interact with the electricity grid:

1. Uncontrolled charging: Vehicles charge at full power from the time when they are plugged in until they either reach a full charge or unplug for their next trip. The power transfer rate is determined only by the type of charger the vehicle is plugged into.

2. V1G controlled charging: Vehicles can alter their charging rates to provide grid services. For instance, vehicles may reduce (or entirely deactivate) their charging during evening peaks and maximize charging during daytime over-generation. We assume that the controllable charging power can range from zero up to the maximum power transfer rate for the type of charger.

3. V2G controlled charging: Vehicles can either charge or discharge at any time step. For instance, vehicles may discharge during evening peaks while charging during daytime over-generation. We assume that the controllable charging power can range from zero to the maximum power transfer rate in either direction depending on the type of charger.

For #2 and #3 above, we implemented the use of two controllers into V2G-Sim:

1. Peak shaving and valley filling (peak-valley) control: Vehicles can maximize their charging during the over-generation period and deactivate charging or discharge during the evening peak. With this control objective, renewables curtailment and growth in the evening peaks can be avoided to the maximum extent; however, up and down ramp rates may remain nearly identical to the original net load.

2. Ramp rate mitigation (ramp) control: Vehicle charging can be adjusted to minimize the ramping rates of the net load. For sharp down-ramp periods, this typically results in vehicles transitioning from discharging to charging during the hours adjacent to the sharp down-ramp. For sharp up-ramp periods, vehicles transition from charging to

discharging during the hours adjacent to the sharp up-ramp. With this control objective, up ramp and down ramp rates are mitigated to the greatest extent.

Specifically, the algorithm optimizes one of the following equations according to the control scheme (Coignard et al., 2018):

Peak-valley control:

$$min. \sum_{t}^{T} \left(Net\ Load(t) + \sum_{i}^{V} P_{charge,i}(t) \right)^2$$

Ramp control:

$$min. \sum_{t}^{T} \left(\Delta Net\ Load(t) + \sum_{i}^{V} \Delta\ P_{charge,i}(t) \right)^2$$

where:

$P_{charge,i}(t)$ = power flow between grid and vehicle i at timestep t

T = number of timesteps

V = number of vehicles

These optimizations are also subject to the following constraints:

$$P_{min,i}(t) \leq P_{charge,i}(t) \leq P_{max,i}(t)$$

$$(SOC_{min,i} - SOC_{init,i}) \times \frac{E_i}{\Delta t} + \sum_{\tau=1}^{t} C_i^{\tau} \leq \sum_{\tau=1}^{t} P_{charge,i}(\tau) \leq (SOC_{max,i} - SOC_{init,i}) \times \frac{E_i}{\Delta t} + \sum_{\tau=1}^{t} C_i^{\tau}$$

$$(SOC_{final,i} - SOC_{init,i}) \times \frac{E_i}{\Delta t} + \sum_{\tau=1}^{T} C_i^{\tau} \leq \sum_{\tau=1}^{T} P_{charge,i}(\tau)$$

where:

$P_{min,i}(t)$ = minimum power flow for vehicle i at timestep t

$P_{max,i}(t)$ = maximum power flow for vehicle i at timestep t

$SOC_{min,i}$ = minimum allowable state of charge for vehicle i

$SOC_{init,i}$ = initial state of charge for vehicle i (at start of simulation)

$SOC_{final,i}$ = final state of charge for vehicle *i* (at end of simulation)

E_i = total battery capacity of vehicle *i*

C_i^{τ} = battery consumption of vehicle *i* at time τ due to driving

Δt = timestep

For more information, see Coignard et al. (2018).

2.5. Renewable energy penetrations

Two sets of scenarios were used that differed only in the amount of renewable electricity present on the MISO grid. These were:

- *MISO Transmission Expansion Planning (MTEP) Distributed and Emerging Technologies (DET) scenario.* Wind generation grows from 8.0% of gross load in 2019 to 14.8% in 2032, while solar PV grows from 0.1% of gross load in 2019 to 7.6% in 2032. Both wind and solar PV generation output as a fraction of total load are held constant from 2033-2039. Maximum renewable generation is therefore 22.4%.

- *Renewable Integration Impact Assessment (RIIA) scenario.* Wind generation grows from 17.0% of gross load in 2023 to 30.8% in 2038, whereas solar PV grows from 1.5% in 2023 to 7.8% in 2038. For earlier years, wind and solar generation is scaled linearly, and for 2039, the fraction of renewable generation is the same as in 2038. The maximum renewable generation fraction is therefore 38.6% of gross load.

Table 5 summarizes these assumptions and provides some additional information. Note that for 2033, the MTEP DET scenario has more than twice the amount of solar PV as in the RIIA scenario, but there is much more wind generation in RIIA, so the overall amount of renewables is higher in the RIIA scenario.

Table 5. Renewable generation assumptions for the MTEP DET and RIIA scenarios.

	2023		2033		2038	
	GWh	**% of load**	**GWh**	**% of load**	**GWh**	**% of load**
Wind						
MTEP DET	68,776	10.0%	105,582	14.8%	107,711	14.8%
RIIA	116,845	17.0%	155,794	21.8%	224,168	30.8%
Solar PV						
MTEP DET	10,713	1.6%	54,192	7.6%	55,284	7.6%
RIIA	10,328	1.5%	26,721	3.7%	57,204	7.8%
Total renewables						
MTEP DET	79,489	11.6%	159,774	22.4%	162,995	22.4%
RIIA	127,173	18.5%	182,515	25.5%	281,372	38.6%
Load	686,613		714,577		728,983	

Source: MISO, with calculations by the authors.

2.6. Charging infrastructure assumptions

2.6.1. Initial assumptions

Our initial assumptions were based on those used in Coignard et al. (2018), which assumed 100% home charging, an increasing fraction of workplace charging, and no public charging. Fig. 13 shows the specific assumptions made. These assumptions were used for all MTEP DET runs and the initial set of RIIA runs.

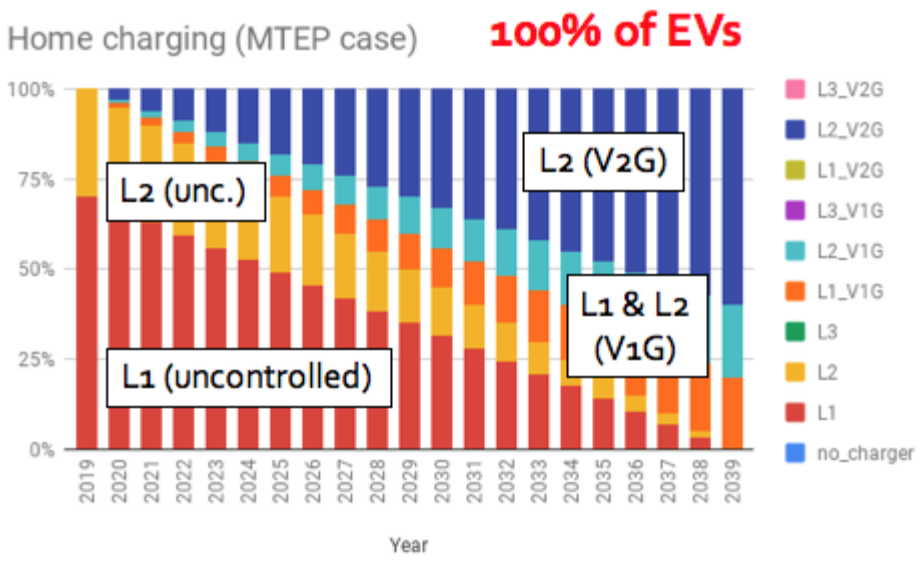

(a)

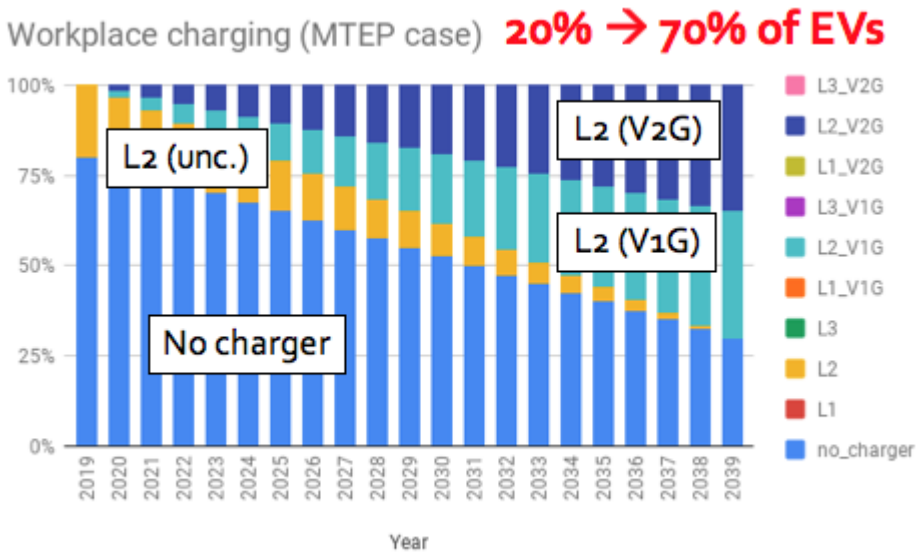

(b)

Fig. 13. Original charging infrastructure assumptions for MTEP and RIIA scenario runs: (a) Home charging, and (b) Workplace charging. No public charging infrastructure was assumed. Source: Coignard et al. (2018), with adjustments made to time period.

2.6.2. Revised assumptions

Revised assumptions were made after consulting with an EV expert (P. MacDougall, pers. commun., 2019) and running scenarios using EVI-Pro (Alternative Fuels Data Center, no date). These revisions consisted of reducing the home charging fraction to 85%, reducing workplace charging to a steady fraction of 1.1%, and introducing public charging. The fractions refer to the number of chargers per EV in the simulation; they do ***not*** refer to the number of vehicles that are able to charge. Because workplace and public charging infrastructure are much more highly utilized than home charging, these smaller numbers of chargers is justified, saving significant

infrastructure cost. Fig. 14 summarizes the assumptions. The revised assumptions were used in the revised RIIA runs and all LRZ runs.

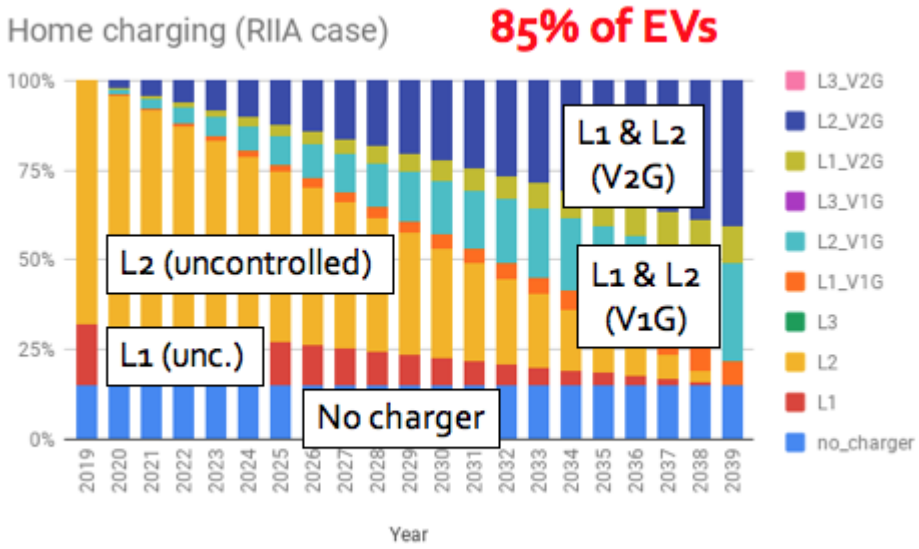

(a)

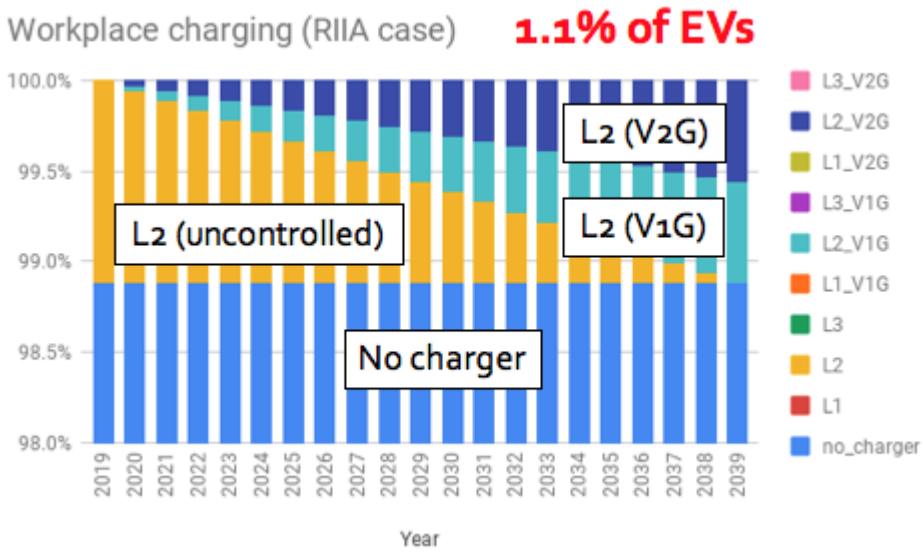

(b)

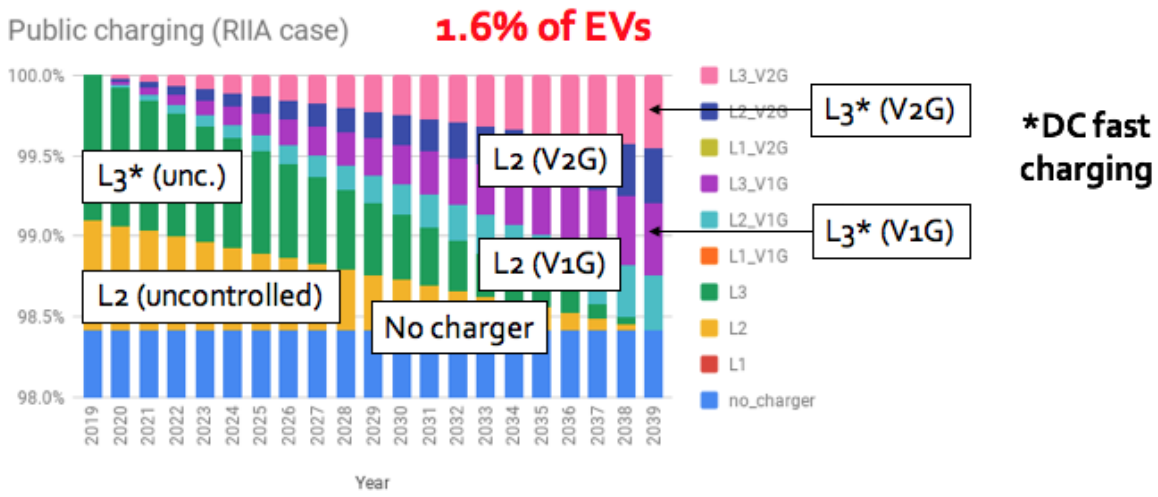

(c)

Fig. 14. Revised charging infrastructure assumptions for all runs: (a) Home charging, (b) Workplace charging, and (c) Public charging. Source: Alternative Fuels Data Center (no date), with assumptions for V1G and V2G charging based on Coignard et al. (2018).

2.7. Cost assumptions

While costs were not the primary focus of our modeling, we did provide some economic estimates associated with managing EV charging. Table 6 provides our estimates of EV charging infrastructure costs for different charging levels and control types, while Table 7 provides estimates of battery degradation associated with different types of charging. We assumed that maintenance/replacement costs were approximated by a five-year lifetime for EV chargers (S. Taber and D. Schlosberg, eMotorWerks, pers. commun., 2018).

Table 6. EV charging infrastructure cost assumptions

Charging level	Control type	Cost ($)
L1	Uncontrolled	200[a]
L2	Uncontrolled	383[b]
L1	V1G	260[c]
L2	V1G	610[d]
L2	V2G	710[e]

Sources:

[a]Based on two products at the same price (Amazon, 2019a, 2019b).

[b]Based on the average of two product prices (Amazon, 2019c, 2019d).

[c]Based on one product (Amazon, 2019e).

[d]Based on the average of four product prices (Amazon 2019f, 2019g, 2019h, 2019i).

[e]We assumed a $100 premium over L2 V1G (S. Taber and D. Schlosberg, eMotorWerks, pers. commun., 2018).

Table 7. Battery degradation assumptions

Control type	Cost ($/day/vehicle)
Uncontrolled	0.730
V1G	0.730
V2G	0.991

Source: Author calculations based on Wang et al. (2016).

2.8. Simulations performed

The following simulations were performed in the course of the project. Each "run" consisted of five or three years, each comprised of twelve one-week simulations representing the months of the year. For the five-year runs, the simulated years were 2020, 2024, 2028, 2032 and 2036. For the three-year runs, the simulated years were 2023, 2033 and 2038. The time step of the simulations was 5 minutes.

2.8.1. MTEP DET simulations

The first set of simulations used load assumptions from the MTEP DET scenario that was supplied to us by MISO. This scenario was used as a starting point or reference, and assumed that renewables grow from 11% in 2023 to 21% in 2032 and beyond. We initially performed five-year runs of these simulations, and initially all four EV penetration scenarios were explored. For the Base EV penetration case, five control strategies (uncontrolled, V1G peak/valley control, V2G peak/valley control, V1G ramp control, and V2G ramp control) were used; for the other three EV penetration cases, only three control strategies (uncontrolled, V1G peak/valley control, and V2G peak/valley control) were used. The runs also used the original charging infrastructure assumptions and the MTEP DET gross load data. A complete set of .res and .dat files was generated for these simulations. A summary of the runs performed is shown in Table 8.

Table 8. Initial MTEP DET runs performed.

Number	EV penetration	Control strategy	Variation
1	Base	Uncontrolled	N/A
2	Base	V1G	Peak/valley control
3	Base	V2G	Peak/valley control
4	Base	V1G	Ramp control
5	Base	V2G	Ramp control
6	Low	Uncontrolled	N/A
7	Low	V1G	Peak/valley control
8	Low	V2G	Peak/valley control

9	High	Uncontrolled	N/A
10	High	V1G	Peak/valley control
11	High	V2G	Peak/valley control
12	Very High	Uncontrolled	N/A
13	Very High	V1G	Peak/valley control
14	Very High	V2G	Peak/valley control
Notes:			
Combination of five-year (2020, 2024, 2028, 2032, 2036) and three-year (2023, 2033, 2038) runs			
Original charging infrastructure			
MTEP DET gross loads			

We also performed some revised MTEP DET runs for a limited number of scenarios, where we used the RIIA rather than MTEP DET gross loads, but retained the original charging infrastructure assumptions. These revised runs were done in order to make a direct comparison between MTEP DET and RIIA runs, where the only differences were in the amount of renewable generation. We reduced the number of runs to just two EV penetration scenarios (Base and Very High), but retained all five control strategies (uncontrolled, V1G peak-valley control, V1G ramp control, V2G peak-valley control, and V2G ramp control). We also only performed these runs for two months (June 2033 and June 2038) for each scenario. As a result, no .res or .dat files were generated because the time series was incomplete. Table 9 shows a summary of the final runs performed.

Table 9. Revised MTEP DET simulations performed (no .res or .dat files generated).

Number	**EV penetration**	**Control strategy**	**Variation**
1	Base	Uncontrolled	N/A
2	Base	V1G	Peak-valley control
3	Base	V2G	Peak-valley control
4	Base	V1G	Ramp control
5	Base	V2G	Ramp control
6	Very High	Uncontrolled	N/A
7	Very High	V1G	Peak-valley control
8	Very High	V2G	Peak-valley control
9	Very High	V1G	Ramp control
10	Very High	V2G	Ramp control

Notes:
June 2033 and 2038 only
Original charging infrastructure
RIIA gross loads

2.8.2. RIIA simulations

The second set of simulations used load assumptions from the RIIA scenario that was supplied to us by MISO. This scenario was used to explore a higher renewable energy future, where renewables grow to 39% by 2038. We exclusively performed three-year runs of these simulations. Initially, as for the MTEP DET simulations, all four EV penetration scenarios were explored, and for the Base EV penetration case, five control strategies (uncontrolled, V1G peak/valley control, V2G peak/valley control, V1G ramp control, and V2G ramp control) were used; for the other three EV penetration cases, only three control strategies (uncontrolled, V1G peak/valley control, and V2G peak/valley control) were used. The runs also used the original charging infrastructure assumptions and the RIIA gross load data. A complete set of .res and .dat files was generated for these simulations. A summary of the initial runs performed is shown in Table 10.

Table 10. Initial RIIA simulations.

Number	**EV penetration**	**Control strategy**	**Variation**
1	Base	Uncontrolled	N/A
2	Base	V1G	Peak/valley control
3	Base	V2G	Peak/valley control
4	Base	V1G	Ramp control
5	Base	V2G	Ramp control
6	Low	Uncontrolled	N/A
7	Low	V1G	Peak/valley control
8	Low	V2G	Peak/valley control
9	High	Uncontrolled	N/A
10	High	V1G	Peak/valley control
11	High	V2G	Peak/valley control
12	Very High	Uncontrolled	N/A
13	Very High	V1G	Peak/valley control
14	Very High	V2G	Peak/valley control

Notes:

Three years (2023, 2033, 2038)
Original charging infrastructure
RIIA gross loads

We also performed some revised RIIA runs for a limited number of scenarios, as for the revised MTEP DET runs. However, the only difference between these runs and the initial RIIA runs was the charging infrastructure assumptions used, in order to make a direct comparison between the two. We reduced the number of runs to just two EV penetration scenarios (Base and Very High), and ran all five control strategies (uncontrolled, V1G peak-valley control, V1G ramp control, V2G peak-valley control, and V2G ramp control) for the Base EV penetration scenario, but only three control strategies (uncontrolled, V1G peak-valley control, and V2G peak-valley control) for the Very High scenario. We also only performed these runs for two months (June 2033 and June 2038) for each scenario. As a result, no .res or .dat files were generated because the time series was incomplete. Table 11 shows a summary of the final runs performed.

Table 11. Revised RIIA simulations (no .res or .dat files generated).

Number	**EV penetration**	**Control strategy**	**Variation**
1	Base	Uncontrolled	N/A
2	Base	V1G	Peak-valley control
3	Base	V2G	Peak-valley control
4	Base	V1G	Ramp control
5	Base	V2G	Ramp control
6	Very High	Uncontrolled	N/A
7	Very High	V1G	Peak-valley control
8	Very High	V2G	Peak-valley control

Notes:
June 2023 and 2038 only
Revised charging infrastructure
RIIA gross loads

2.8.3. LRZ simulations

The final set of simulations were the LRZ simulations, where we focused exclusively on two LRZs: 1 (primarily Minnesota, with parts of North Dakota, South Dakota, Wisconsin and Montana) and 7 (Michigan). Gross loads and renewable generation by LRZ were supplied to us by MISO for a hypothetical 42% renewable generation scenario in 2017 (an approximation of the RIIA scenario that reaches 39% in 2038), from which we constructed net load curves. The

LRZ simulations were used to explore variations among EV penetrations and renewable generation, shown in Table 12 and visualized in Fig. 15. We selected these two LRZs as they represented interesting bounds in a two-dimensional space; the other bound, at low EV penetrations and low renewable generation, is less interesting from the perspective of controlled charging. We exclusively performed three-year runs of these simulations.

Table 12. Load (2017), renewable generation (hypothetical for 2017; approximates 2038), cumulative EV sales (2011-2018) and EV sales per TWh of load by LRZ

LRZ	Load (TWh)	Renewables (TWh)	Renewable fraction	Fraction of MISO load	EV sales (2011-2018)	EV sales per TWh of load
1	94.5	80.8	86%	14.1%	9,514	101
2	63.5	16.1	25%	9.5%	7,847	124
3	48.1	85.2	177%	7.2%	2,529	53
4	48.1	21.2	44%	7.2%	4,971	103
5	37.0	6.8	18%	5.5%	2,882	78
6	99.0	21.5	22%	14.8%	4,870	49
7	98.4	25.9	26%	14.7%	17,426	177
8	40.1	7.9	20%	6.0%	914	23
9	118.1	11.0	9%	17.6%	3,283	28
10	23.5	4.9	21%	3.5%	334	14
All	670.4	281.4	42%	100.0%	54,569	81

Source: MISO and Auto Alliance (2019), with analysis by the authors.

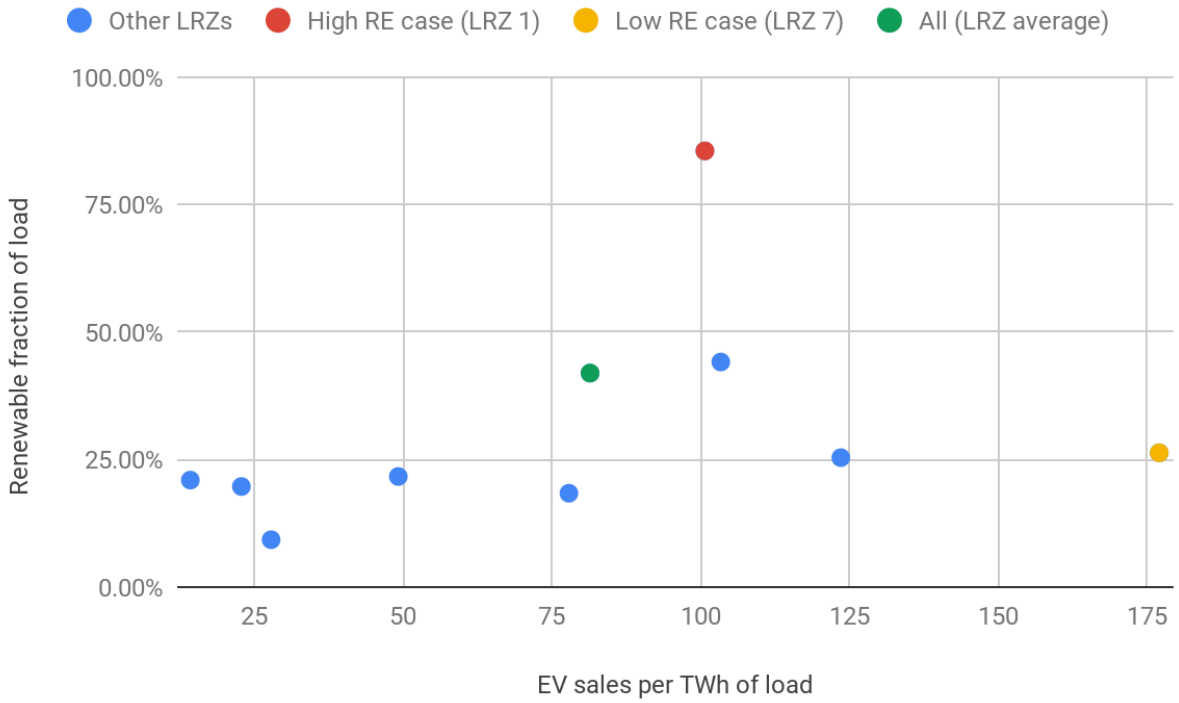

Fig. 15. Scatterplot showing the renewable fraction of load (hypothetical for 2017; approximates 2038) vs. EV sales (2011-2018) per TWh of load for each LRZ. Note: LRZ 3 not shown (>100% renewable fraction of load). Source: MISO and Auto Alliance (2019), with analysis by the authors.

We performed three-year runs for the LRZ simulations. Like the final MTEP DET and RIIA simulations, we performed two EV penetration scenarios (Base and Very High), and three control strategies (uncontrolled, V1G ramp control, and V2G ramp control). We also utilized revised charging infrastructure assumptions, and used RIIA gross loads (scaled to the annual demand for each LRZ). A complete set of .res and .dat files was generated for these simulations. Table 13 shows a summary of the final runs performed.

Table 13. LRZ simulations performed.

Number	EV penetration	Control strategy	Variation
1	Base	Uncontrolled	N/A
2	Base	V1G	Ramp control
3	Base	V2G	Ramp control
4	Very High	Uncontrolled	N/A
5	Very High	V1G	Ramp control
6	Very High	V2G	Ramp control

Notes:
Three years (2023, 2033, 2038)
Revised charging infrastructure
RIIA gross loads

2.9. Computational resource constraints

Simulating a set of realistic EVs interacting with an electric grid is a demanding computational task that required increasing amounts of computational time as the number of simulated EVs increased. As an example, to simulate one year in the Base case using peak-valley control optimization required between 1 hour (for the 2020 simulation) and 2 hours (for the 2036 simulation). For cases with higher numbers of EVs, the simulations took longer. Also, for the ramp control optimizations, the simulations took approximately three times as long as for peak-valley control. Therefore, running each year of the simulation, let alone every day of every year, was out of the question with the computational resources available to us. We also did not perform both peak-valley and ramp control optimizations for each scenario combination, but after an initial exploration of both control optimizations, chose to focus on ramp control as a more "representative" control algorithm for the real world.

As a result, we chose to interpolate our results among five (and, for the bulk of the runs, three) simulated years for key output parameters (total energy, peak load, cost, etc.) by scaling our results for intervening years by the numbers of EVs as prescribed by the EV penetration scenario.

For example, for simulated result for 2023 and 2033, in order to scale the load profile to 2030, two steps are used. If $Load_{2033}$represents the load profiles in the year 2033, $EVLoad_{2030}$ represents the corrected load after considering the EV number. First, we roughly scale the load based using the equation:

$$Load_{2030} = \frac{2033-2030}{2033-2023} \cdot Load_{2023} + \frac{2030-2023}{2033-2023} \cdot Load_{2033}$$

Then, we accurately scale the load based on the numbers of EVs:

$$EVLoad_{2030} = \left(\frac{Load_{2033}}{EV_{2033}} / \frac{Load_{2030}}{EV_{2030}}\right) \cdot Load_{2030}$$

3. Results and discussion

3.1. MISO net load shape without EVs

We begin by presenting the basic MISO net load shape (e.g., without any EV charging). This is constructed by subtracting the wind and solar generation from the MISO gross load (taken in this example from the MTEP DET scenario). Fig. 16 shows these four datasets in 2012, from

which our simulation data for future years was constructed. Four single weeks of data are shown, representing the winter, spring, summer and fall seasons. Starting with the gross load curves, one can clearly see the daily (or "diurnal") variation in load that is lowest after midnight and peaks once or twice during the day. It is a general pattern in the MISO region that the gross load experiences a single peak during the summer, and two distinct morning and evening peaks in the other three seasons, though in certain weeks spring can also display a single daily peak. Both the daily peaks and valleys are also highest during the summer, and lowest in the fall; winter and spring tend to fall somewhere in between, and in certain weeks the winter peaks can be larger than those in spring. For the example summer week (Sunday, July 29 through Saturday, August 4), one can also clearly see lower peak demand on the weekend days as compared to weekdays, though these differences are largely masked by larger variations in weather in most weeks.

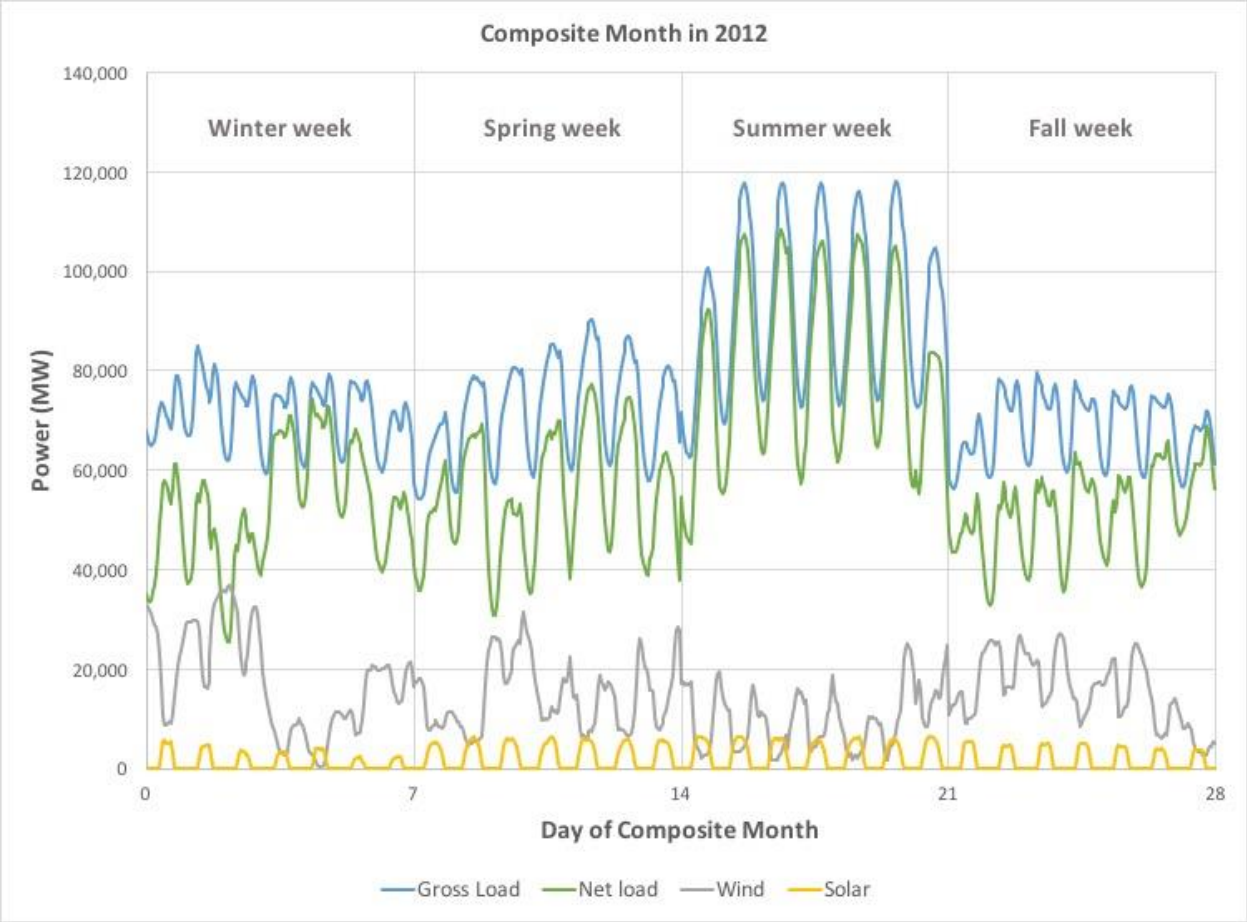

Fig. 16. Example MISO gross load curve, net load curve, and wind and solar generation for four weeks in 2012 (starting January 29, April 29, July 29 and October 28 and labeled Winter, Spring, Summer and Fall weeks, respectively). Source: MISO, with analysis by the authors.

Turning to the wind generation curve, several things are prominent. First, there is a lot more variation over a given week than in the gross load curves, with no clear seasonal pattern other than slightly lower average generation in the summer (this is not immediately obvious from the

Figure, but is generally true throughout the season). Second, there is generally a diurnal pattern that peaks at night and falls to its lowest levels during the day (and is therefore anticorrelated with peak demand), though there are frequent exceptions. Third, the troughs in wind generation output some days can be larger than the peaks other days; in other words, output is highly variable over a period of several hours to days.

By contrast, the solar generation curve is much more predictable: peaking during the day (slightly preceding the gross demand peak in time) and zero at night, with fairly similar peak output from one day to the next, although it is more variable in the winter as can be seen by larger differences in peak out between, for instance, days 5 and 6. Also, the peak solar output is highest during the spring and summer, and lowest in fall and winter. The absolute peak solar output is also much lower than the peak wind output, due to the relatively small amount of installed solar PV in 2012, but this amount can be changed in future years when assuming a larger total solar installed capacity.

Subtracting the wind and solar generation from the MISO gross load yields the MISO net load. While the net load preserves most of the features of the gross load, overall there is more variation day-to-day, in particular due to the variable nature of wind generation. The diurnal peak-to-valley differences are also larger, due to the largely anticorrelated gross load and wind generation peaks. Finally, the daily solar generation peak occurring in the middle of the day can result in a deeper trough in between the morning and evening load peaks (or a slight reduction in the single peak in summer months), though this effect tends to be wiped out by much larger variations in wind generation.

In modifying these datasets for our simulations between 2019 and 2039, the gross load curve was simply scaled uniformly upward by a factor that varied with the year, amounting to a 0.4%/yr load growth. The wind and solar generation curves were also scaled upward in future years according to the assumptions about renewable energy generation (see Renewable energy penetrations section for details). The net load curves are therefore different in each year of our simulation, and between the MTEP and RIIA scenarios. It is this starting point from which simulations with EV charging then proceeds.

3.2. MTEP DET simulations

We used the MTEP DET simulations as our reference case. We begin by illustrating how the net load curves change when EVs are added under different charging protocols. See Fig. 17. For this example, taken from February 2028 where there are 1.01 million EVs in our Base scenario, the uncontrolled charging case (black) slightly exacerbates the load peaks each day, as charging tends to coincide with early evening. For the V1G control strategy simulations—both peak-valley control (cyan) and ramp control (green)—we can see small reductions in those peaks each day, approaching the no-EV base case (blue); there are also small increases in the valley loads with these two control strategies, indicating a shifting of load from peak to valley periods.

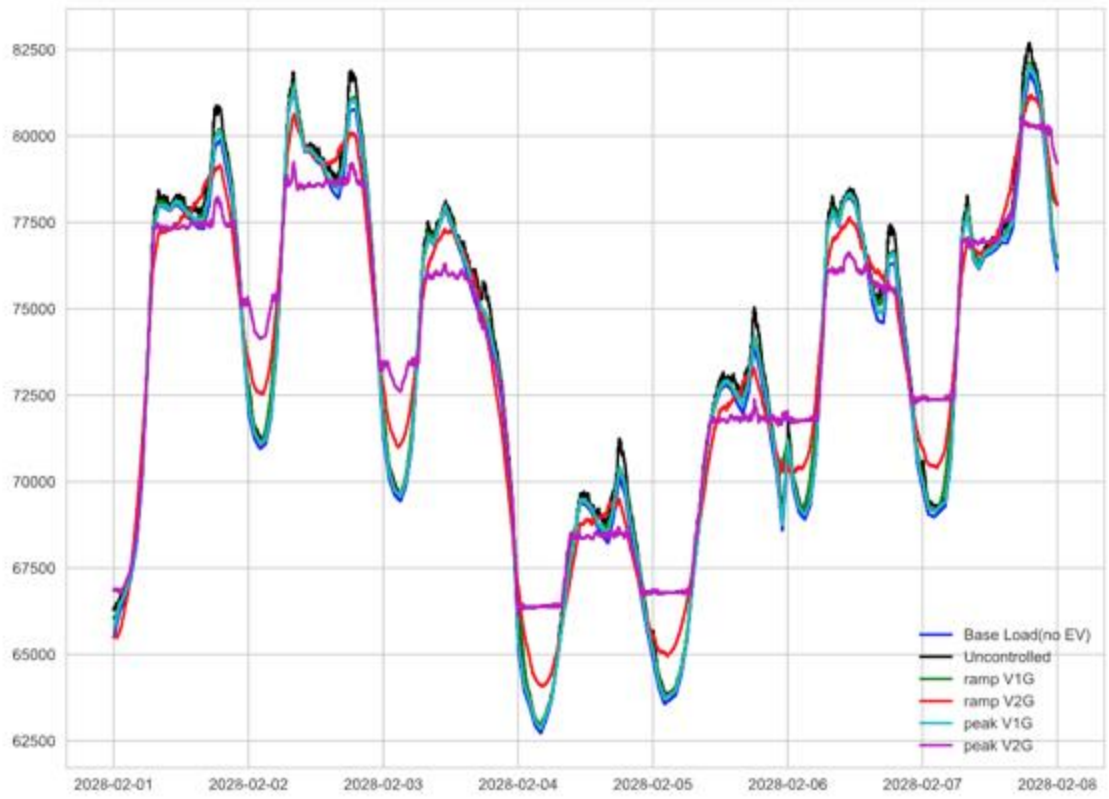

Fig. 17. Controlled charging effects for the initial MTEP DET runs, Base scenario, February 2028. *Y-axis units are MW.* Source: Author calculations.

Much larger changes occur for the V2G control strategy simulations, however. For peak-valley control (magenta), peaks and valleys are nearly flat, with sharp transitions in between, while for ramp control (red), slopes are noticeably reduced, which also has an effect on reducing peaks and filling in valleys, though not as much as in the peak-valley control strategy. While it is difficult to make out the effects of shallower slopes in the up- and down-ramp segments of the time series, this will be much more apparent below when the number of EVs is larger.

Fig. 18 shows the same week in February 2032 when the number of EVs has grown to 2.16 million. As a result, the size of the uncontrolled charging peaks are noticeably larger. There is also a larger number of controlled charging stations in the simulation, which makes the effects of both V1G and V2G controlled charging larger. For the V1G control strategy simulations (cyan and green), one can clearly see reductions in the daily peaks each day, approaching the no-EV case (blue); as for the 2028 example, there are also small increases in the valley loads.

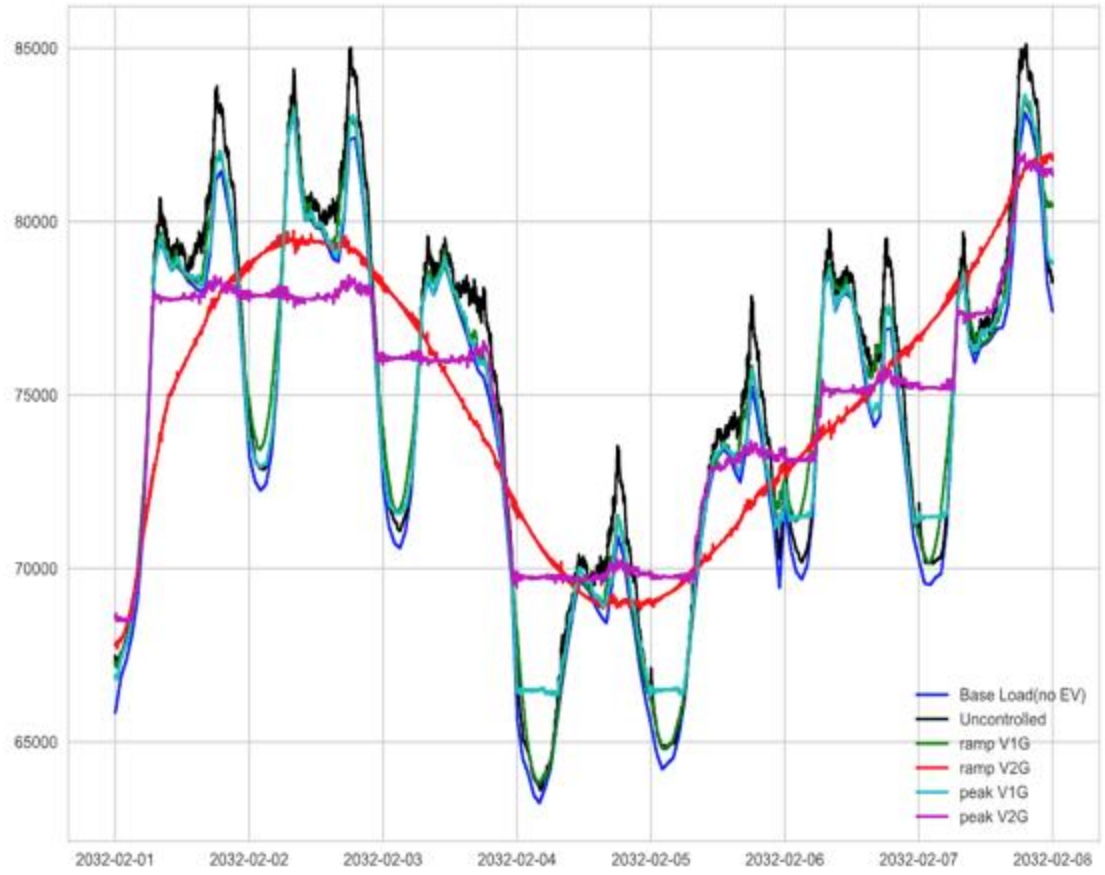

Fig. 18. Controlled charging effects for the initial MTEP DET runs, Base scenario, February 2032. Y-axis units are MW. Source: Author calculations.

Very dramatic changes now occur for the V2G control strategy simulations. For peak-valley control (magenta), peaks and valleys are nearly flat, with sharp transitions in between; in fact, there is so much EV capacity that for most days, peaks and valleys have merged into a single flat load period that in more than one occasion extends over a 24-hour period. For ramp control (red), even larger changes have occurred, with slopes reduced to the point where the load slowly grows toward a gentle peak on February 2, decreases into a gently-sloping valley on February 4, then climbs toward an overall peak for the week at the beginning of February 8. In other words, the ramp control strategy has become a multi-day optimization.

We have observed this phenomenon to occur in other months and EV penetration scenarios, but the onset appears to depend on several factors (number of EVs, number of V2G-capable chargers, and shape of the net load curve) that we have not yet fully characterized. Understanding the conditions for which multi-day optimization emerges will be the subject of future investigation.

Another example of the transition from single-day to multi-day optimization is illustrated in Fig. 19, for a different month (June) in 2033. Here we see that the transition to multi-day optimization has mostly occurred for the V2G peak-valley control optimization (magenta), but with noticeable

peaks remaining most days. By contrast, the V2G ramp control optimization (red) is unable to perform multi-day optimization, so instead tries to slowly vary the load among remaining peaks as smoothly as possible.

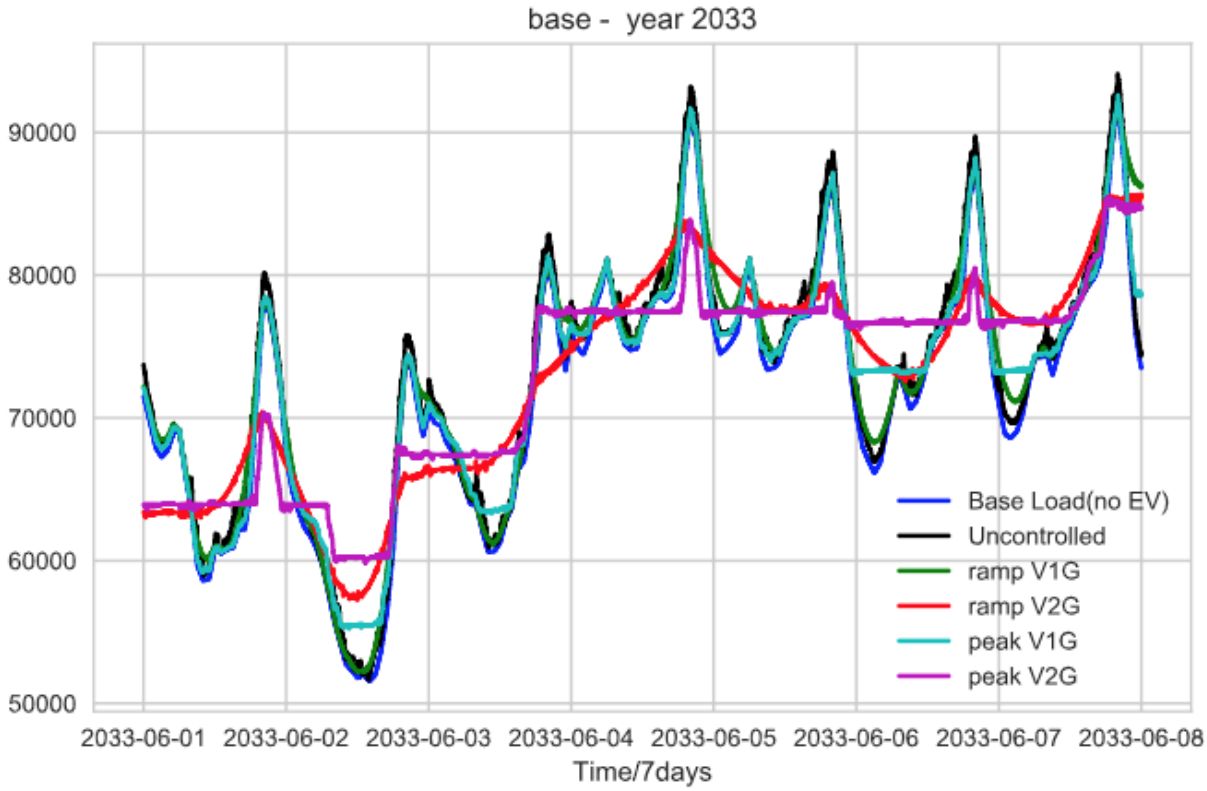

Fig. 19. Base EV penetration scenario for June 2033. Number of EVs is ~2.5 million. Y-axis units are MW. Source: Author calculations.

By 2038, the same scenario now has almost double the number of EVs, and has completely transitioned to multi-day optimization for both the V2G peak-valley control (magenta) and ramp control (red) strategies (see Fig. 20). Even the V1G optimizations are able to nearly completely mitigate the EV loads away from the peaks toward periods of lower demand, as evidenced from the flat valleys in the V1G peak-valley control strategy (cyan) each night, and the V1G ramp control strategy (green) is able to smoothly vary load between peaks—see for example nighttime load between June 5 and 6.

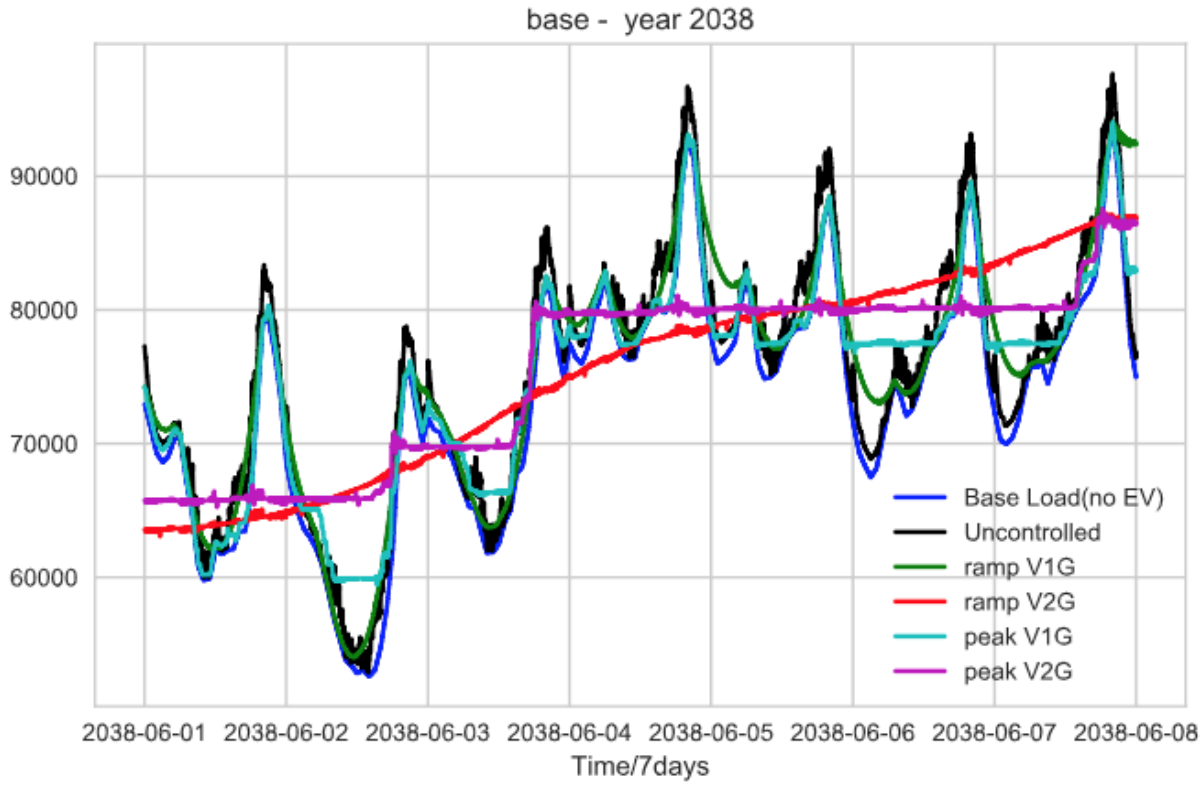

Fig. 20. Base EV penetration scenario for June 2038. Number of EVs is ~4.7 million. Y-axis units are MW. Source: Author calculations.

Finally, Fig. 21 shows the same month and year as in Fig. 20 but for the Very High EV penetration scenario that has more than seven times the number of EVs. Here we see a very large amount of additional load in the uncontrolled charging scenario (black) that significantly offsets it from the no-EV load (blue), but both the V1G and V2G control strategies are able to flatten this load into nearly a constant demand across the entire week (note that only peak-valley control runs were performed for this EV penetration case, but we expect the effects of ramp control to be similar in extent, if somewhat different in resulting load shape). Because there is so much EV capacity, the V1G strategy is also nearly indistinguishable from the V2G strategy, with the only places of significant disagreement being two peaks in V1G case (cyan) that are located where peaks in the no-EV case (blue) lie above the average V1G load (see e.g., evenings of June 1 and 4).

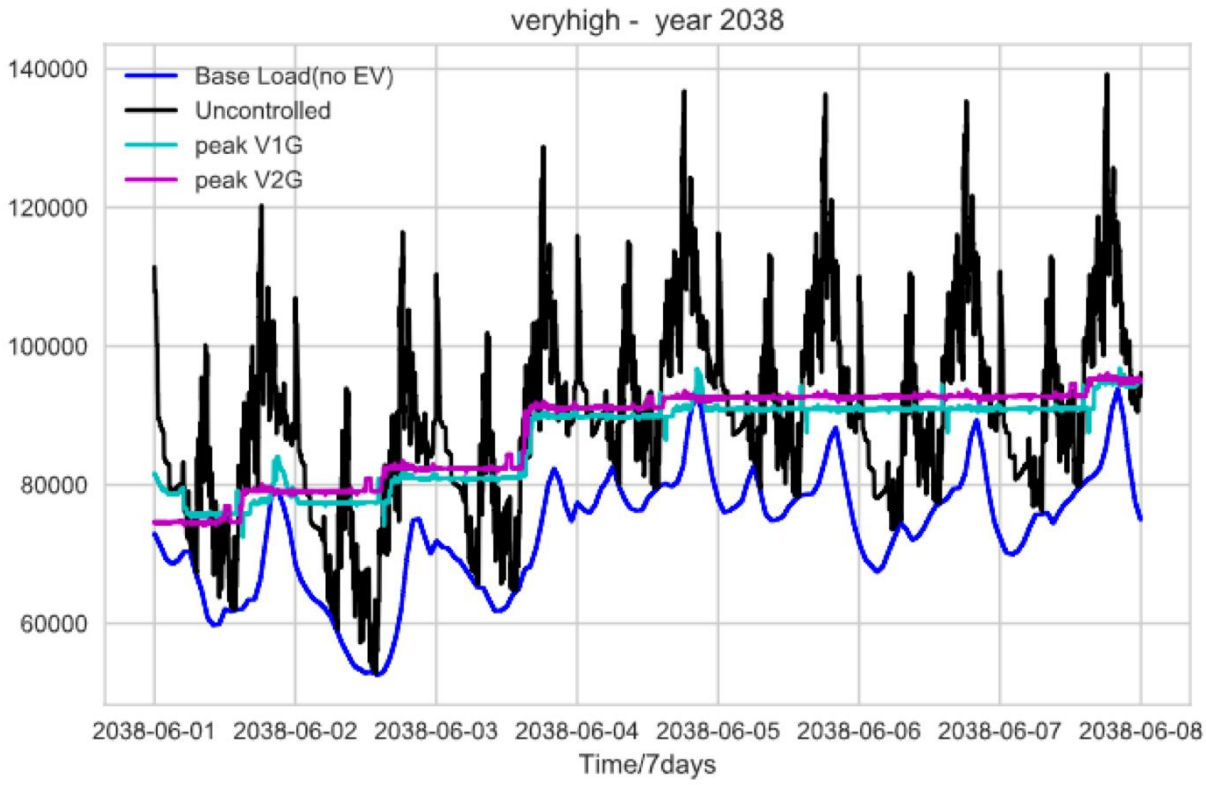

Fig. 21. Very high EV penetration scenario for June 2038. Number of EVs is ~34 million. Y-axis units are MW. Source: Author calculations.

3.3. RIIA vs. MTEP DET simulations

Here we compare the final high renewables (RIIA) results with the lower renewables (MTEP DET) results. All other differences, including gross load curves, charging infrastructure and numbers of EVs, are identical. We present two pairs of results for June 2038 to highlight the impact of higher renewables on the optimization: the Base EV penetration and the Very High EV penetration scenarios.

Fig. 22 shows the MTEP DET result for the Base EV case in June 2038, whereas Fig. 23 shows the RIIA result. All five EV charging optimations (uncontrolled, V1G peak/valley, V1G ramp, V2G peak/valley, and V2G ramp) are shown. To begin with, the differences in the uncontrolled EV charging (black) load curves are significant in terms of peak and valleys loads: the MTEP DET scenarios consistently show higher peaks as well as higher valleys. For example, the highest load level in Fig. 22 is ~90,000 MW (June 6), whereas in Fig. 23 it is ~84,000 MW (June 5). Moreover, the lowest load level in Fig. 22 is ~51,000 MW (June 4 and 6), whereas in Fig. 23 it is ~31,000 MW (June 7). These large differences are due to higher levels of renewables in the RIIA simulations.

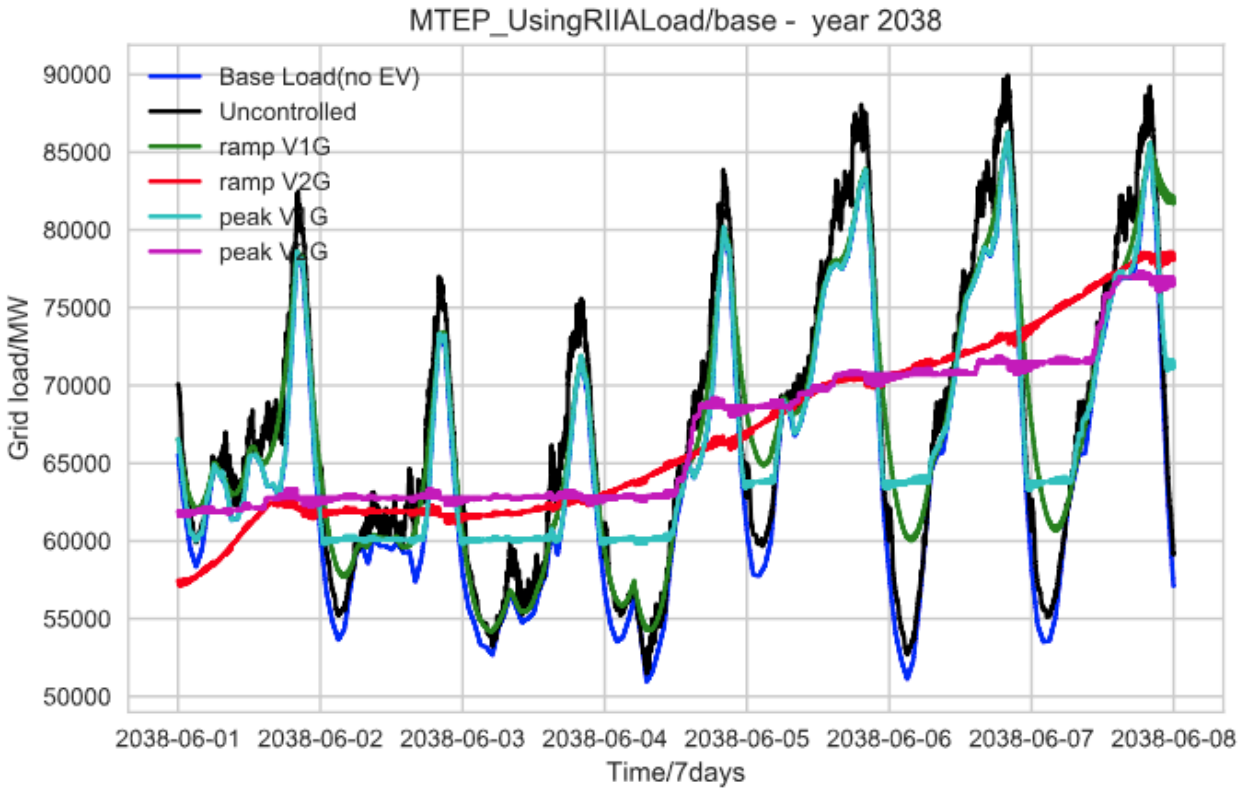

Fig. 22. Base EV penetration for revised MTEP DET scenario in June 2038. Source: Author calculations.

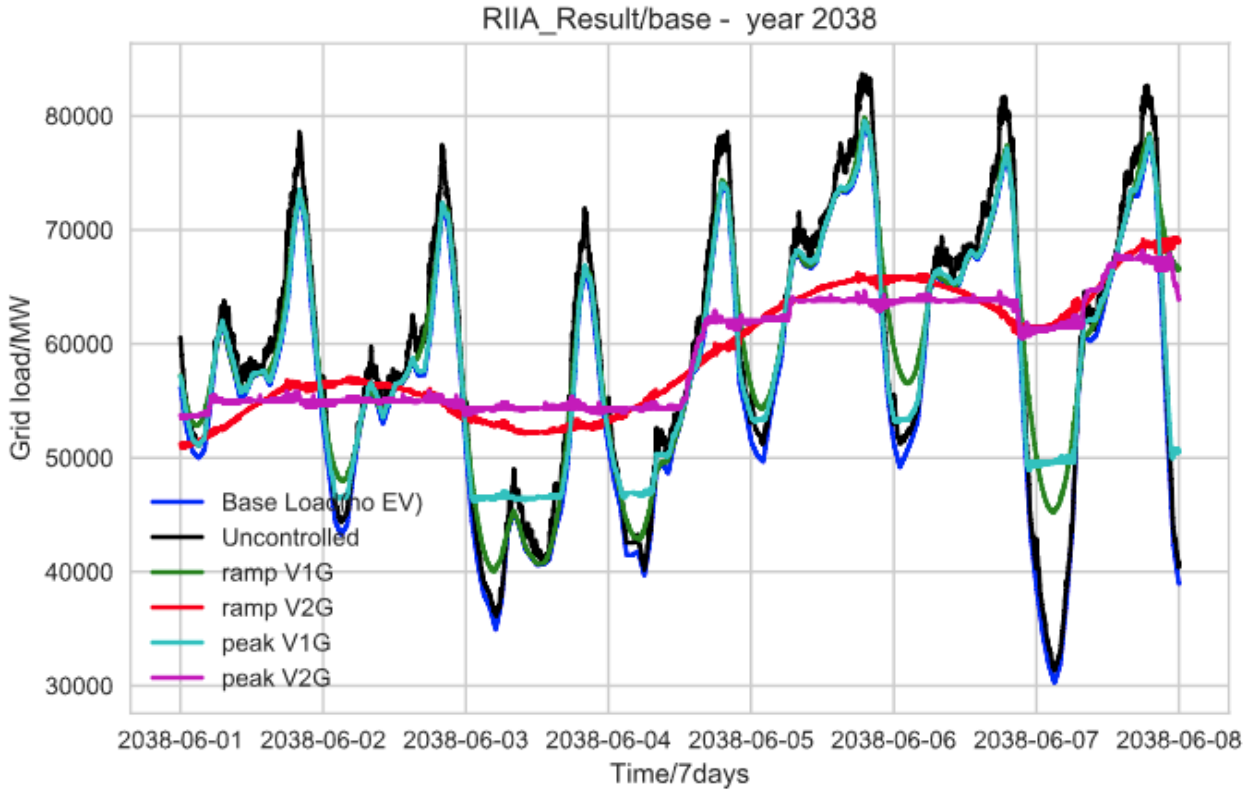

Fig. 23. Base EV penetration for initial RIIA scenario in June 2038. Source: Author calculations.

As a result, the optimizations obtain somewhat different results, though the differences are actually quite minor. For instance, for the peak-valley V1G control (cyan), the filling in of the valleys in Fig. 22 each day is flatter over a longer time period than in Fig. 23. The lowest valley load is also higher in Fig. 22 (~60,000 MW) than in Fig. 23 (~47,000 MW). Otherwise, the basic shapes of the optimizations (for both V1G and V2G, and both peak-valley and ramp optimizations) are quite similar. For the ramp V2G optimization, one can see slightly more "wave" over the course of the week in Fig. 23 than in Fig. 22, indicating a greater need to modulate output in response to deeper peak-valley load differences each day, but other differences are hard to spot.

For the Very High EV penetration case, the differences are even less pronounced between the MTEP DET and RIIA scenarios, as the amount of EV load in the simulations dominates. Figs. 24 and 25 show the results of both, respectively, for June 2038. One can see that both the V1G and V2G solutions are virtually the same and difficult to distinguish between the MTEP DET (Fig. 24) and RIIA (Fig. 25) scenarios: all four show flat outputs over multiple days, with small upward steps as the week proceeds. While the exact points in time where these transitions take place vary between the two scenarios, the resulting behavior is very similar. The most significant difference is in overall load level: for the peak V2G optimization (magenta) on June 7, the MTEP DET scenario load is ~85,000 MW (Fig. 24), whereas the RIIA scenario load is ~75,000 MW (Fig. 25).

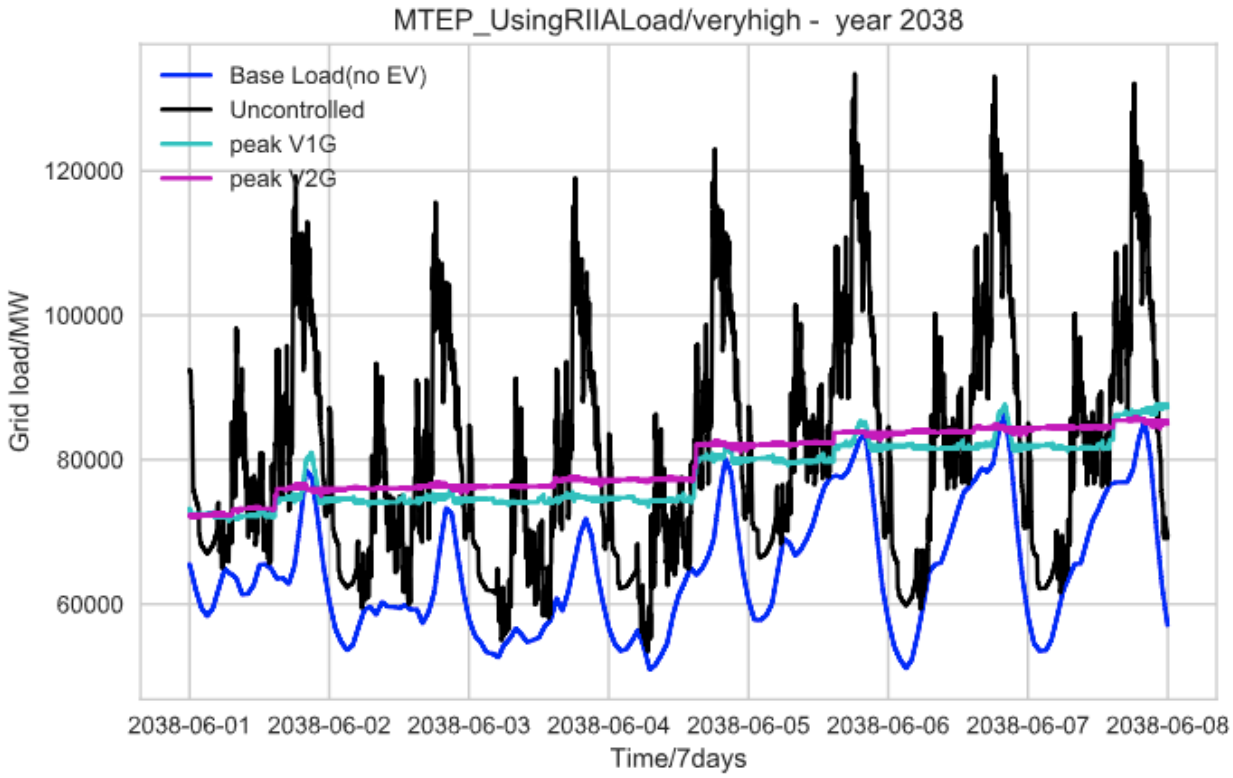

Fig. 24. Very High EV penetration for revised MTEP DET scenario in June 2038. Source: Author calculations.

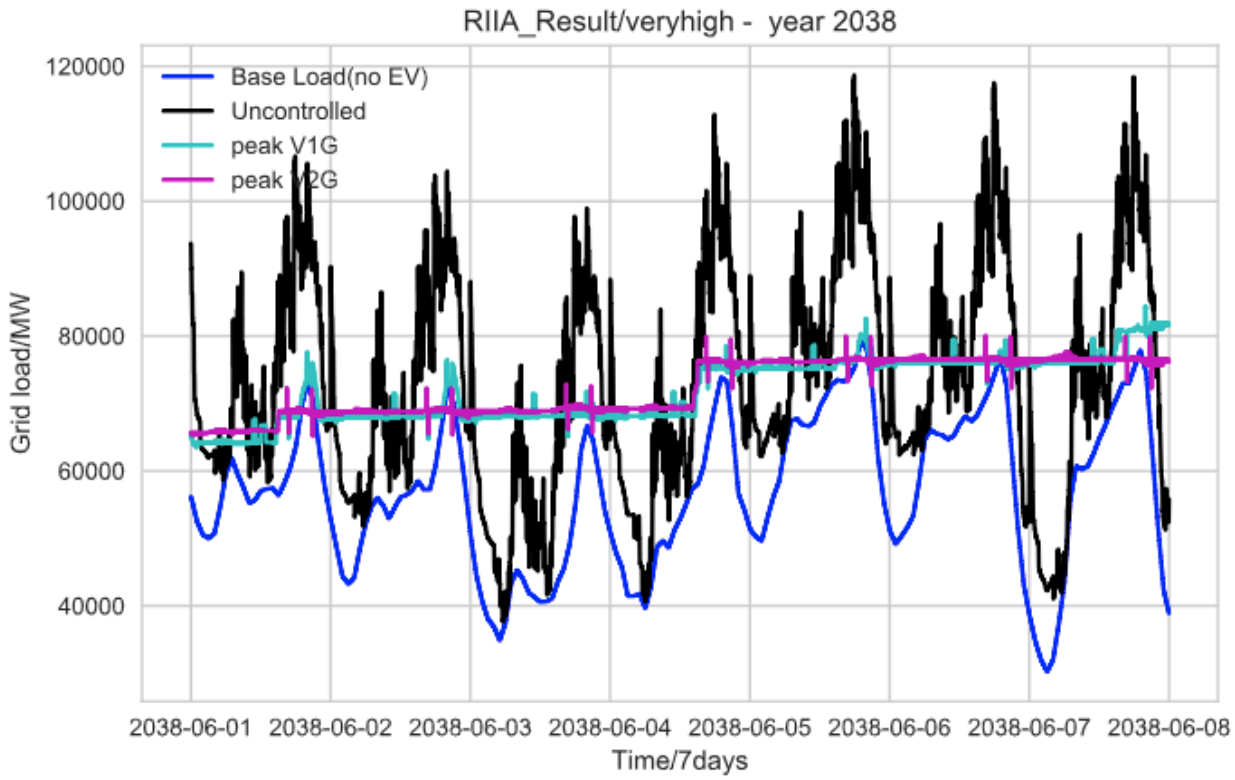

Fig. 25. Very High EV penetration for initial RIIA scenario in June 2038. Source: Author calculations.

3.4. Initial vs. revised charging infrastructure

Here we compare the two sets of RIIA runs to explore the impact of changing the charging infrastructure assumptions. Figs. 26 and 27 show the Base EV penetration in June 2038 with initial and revised charging infrastructure assumptions, respectively. (Note: Fig. 26 is the same as Fig. 23.) Overall, while the differences in V1G charging profiles are fairly small, we see a larger extent of load shifting among the V2G charging profiles in the initial charging infrastructure configuration as compared with revised infrastructure. Whereas we see a transition to multi-day optimization for both sets of V2G control strategies in Fig. 26, the optimizations for V2G are almost exclusively single-day (with the exception of the peak V2G optimization on June 1-2) in Fig. 27. As a result, the day-to-day load excursions are smaller with the initial charging infrastructure than with revised infrastructure, indicating that there is less load shifting capacity available with revised infrastructure. This is consistent with our downward revisions in the amount of home and, especially, workplace charging. The addition of public charging in the revised charging infrastructure assumptions are apparently insufficient to compensate for these reductions, resulting in less load flexibility of the EV fleet for a given level of EV penetration. However, the load-shifting capacity in the Base EV penetration scenario by 2038 is still very significant, and for the Very High EV penetration scenario (not shown), the

transition to multi-day optimization in V2G control strategies still takes place with revised charging infrastructure assumptions.

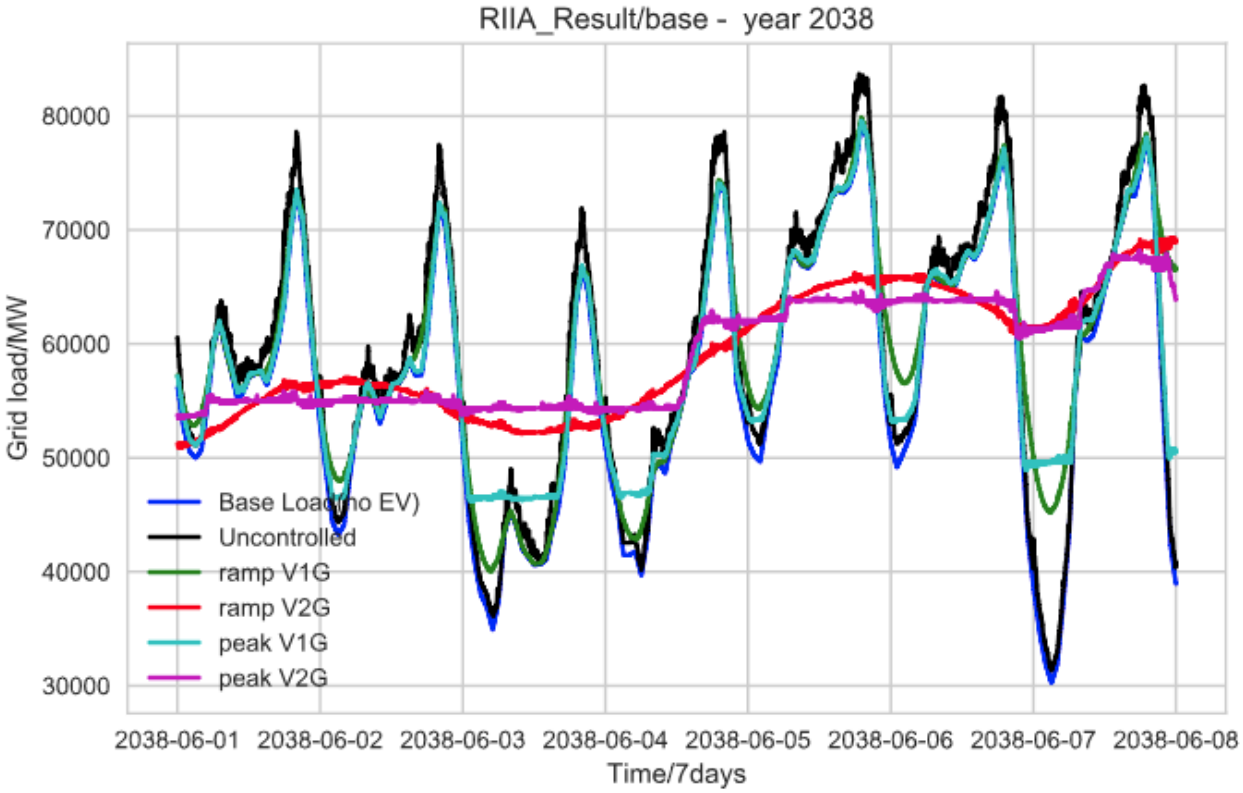

Fig. 26. Base EV penetration for initial RIIA scenario (with initial charging infrastructure assumptions) in June 2038. Note: This figure is the same as Fig. 23. Source: Author calculations.

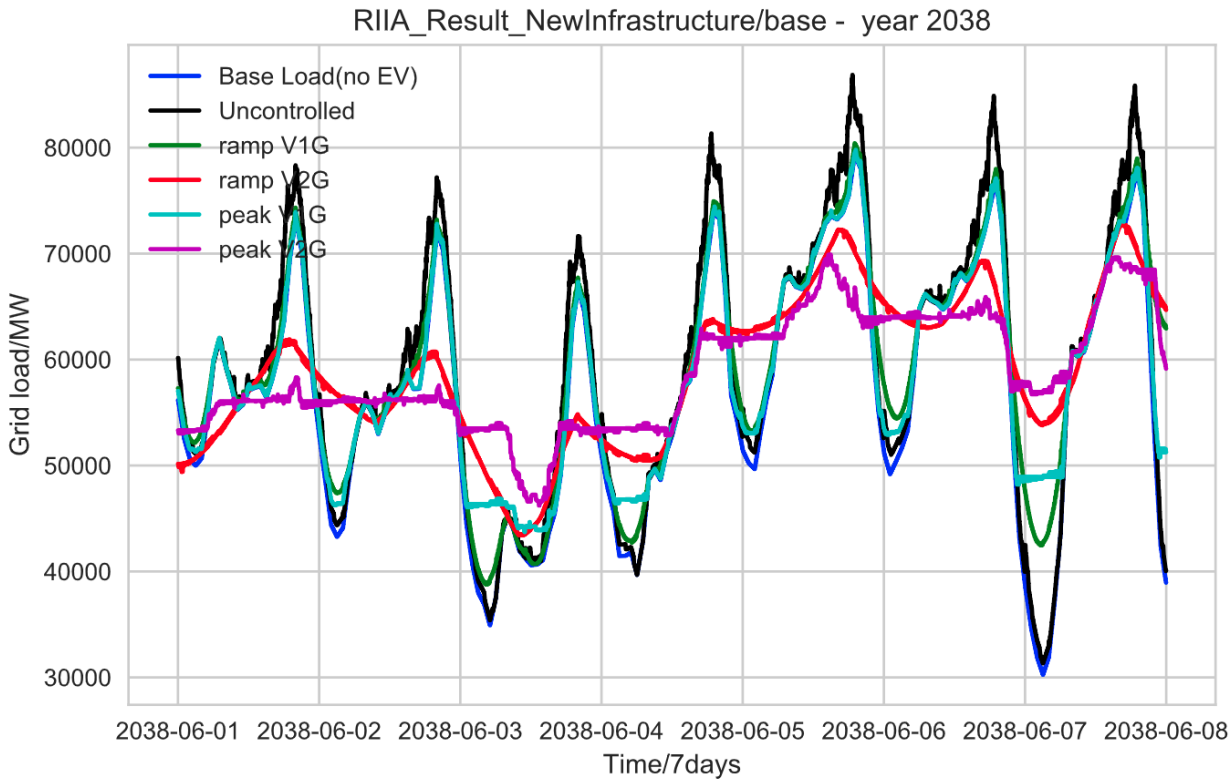

Fig. 27. Base EV penetration for revised RIIA scenario (with revised charging infrastructure assumptions) in June 2038. Source: Author calculations.

3.5. LRZ simulations

We first present results for the LRZ 1 simulations, where renewables produce 86% of gross load annually. Figs. 28 and 29 show the Base and Very High EV penetration scenarios, respectively, in June 2033. While the Base scenario (Fig. 28) in the V1G case (green) shows very minor changes as compared with the uncontrolled charging case (black), the V2G case (red) shows more prominent reductions in slope, as well as significant peak shaving and valley filling each day. Note that net load is sometimes negative, e.g., renewable generation falls below zero during a portion of the day on June 7 in all optimizations [and by >1,000 MW in the no-EV case (blue)], indicating that renewable generation exceeds gross load (including that of added EVs) during that period. In actual practice, this would result in either an export of excess renewable generation to other LRZs, or renewables curtailment.

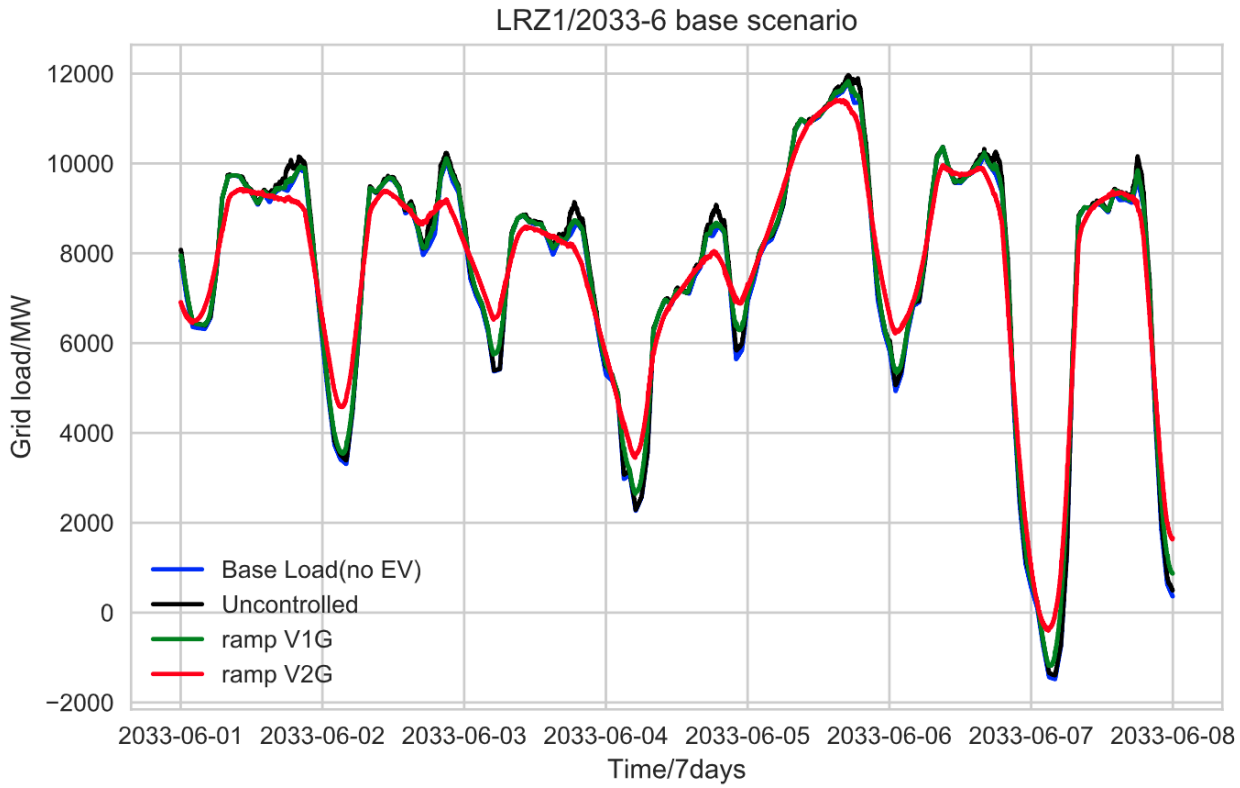

Fig. 28. Base EV penetration scenario for LRZ 1 in June 2033. Source: Author calculations.

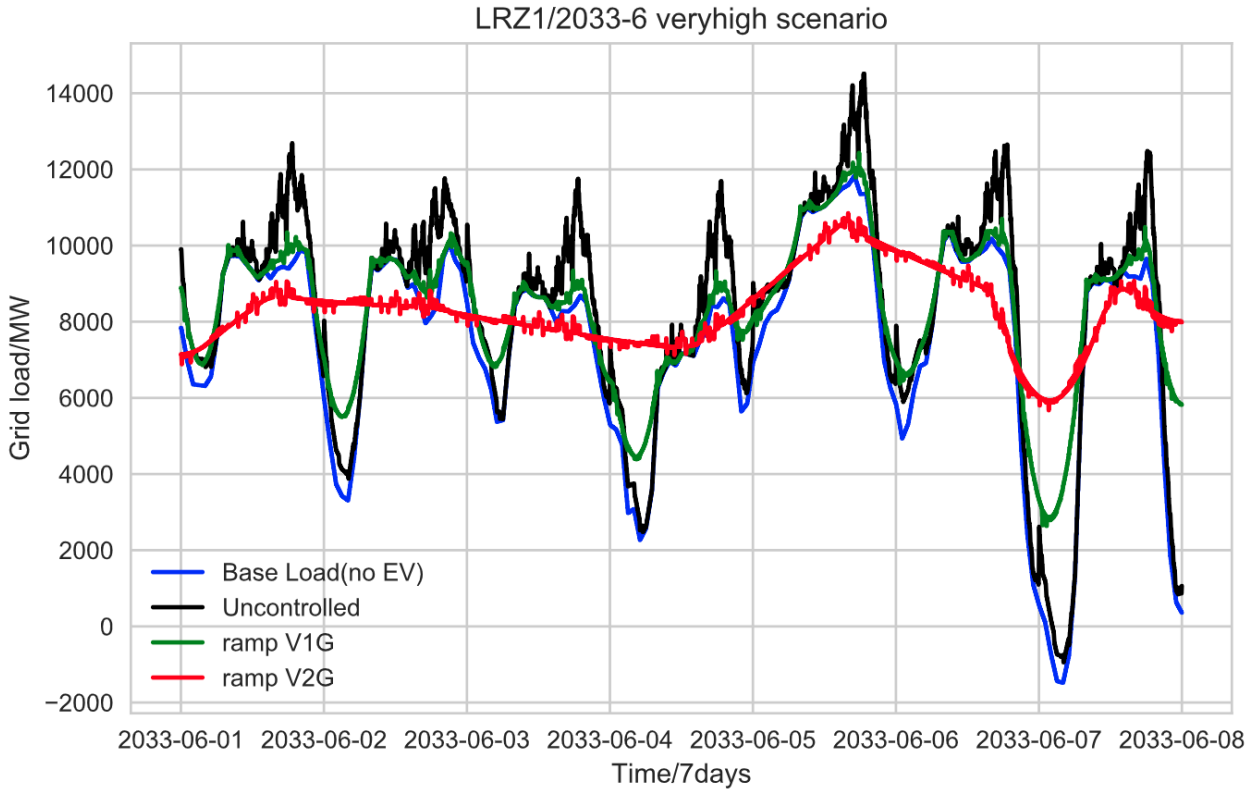

Fig. 29. Very High EV penetration scenario for LRZ 1 in June 2033. Source: Author calculations.

By comparison, the Very High scenario (Fig. 29) shows much larger amounts of load shaping, with the V1G case (green) reducing daily peaks almost to the levels in the no-EV case (blue) while partially filling in nighttime valleys. The V2G case (red) has so much load shaping capacity that the load profile across the week is substantially smoothed, with gently sloping changes in loads across multiple days—dramatically different from the uncontrolled optimization case (black). Note that the "spiky" texture in the V1G and V2G optimized results are due to the limited numbers of EVs in the simulation and not any real physical effect of the optimization. Also, both the V1G and V2G optimization cases have raised the net load above zero throughout the entire week of the simulation, obviating the need for either export of excess renewable generation or curtailment.

Figs. 30 and 31 show the same simulations for June 2038. For the Base EV penetration scenario (Fig. 30), we find more substantial modifications to the base load curve for both the V1G and V2G optimization schemes, but the optimizations are basically still limited to a single day. The other difference of note is that the negative net load excursions are now deeper, e.g., in the no-EV and uncontrolled charging cases, it dips below -7,000 MW in the early morning of June 7, and makes less pronounced excursions below zero during the evenings of June 6 and 7, as well as momentarily on June 4.

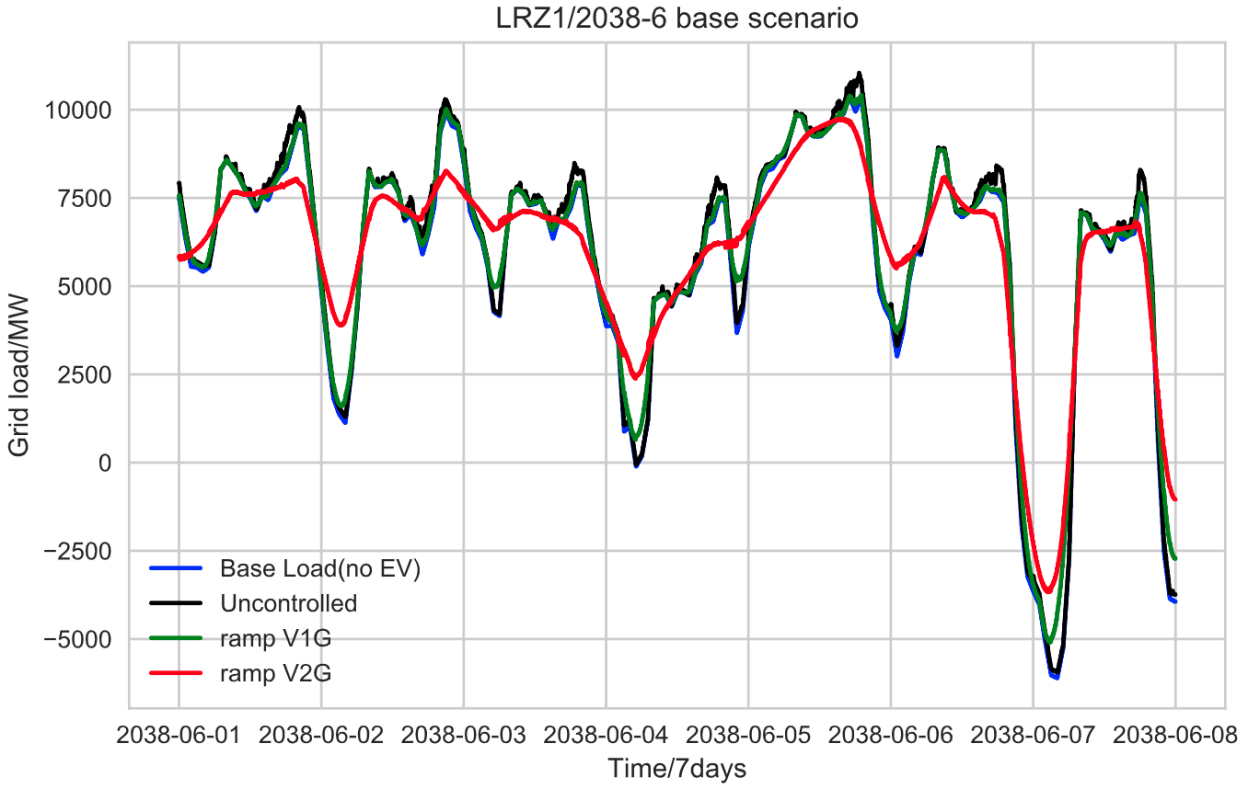

Fig. 30. Base EV penetration scenario for LRZ 1 in June 2038. Source: Author calculations.

By contrast, in the Very High scenario (Fig. 31), while the V1G case (green) appears very similar to that of June 2033 (see Fig. 29) except for deeper filling of valley loads, the V2G case

(red) displays a net load curve that is flatter across the entire week than in the June 2033 V2G case.

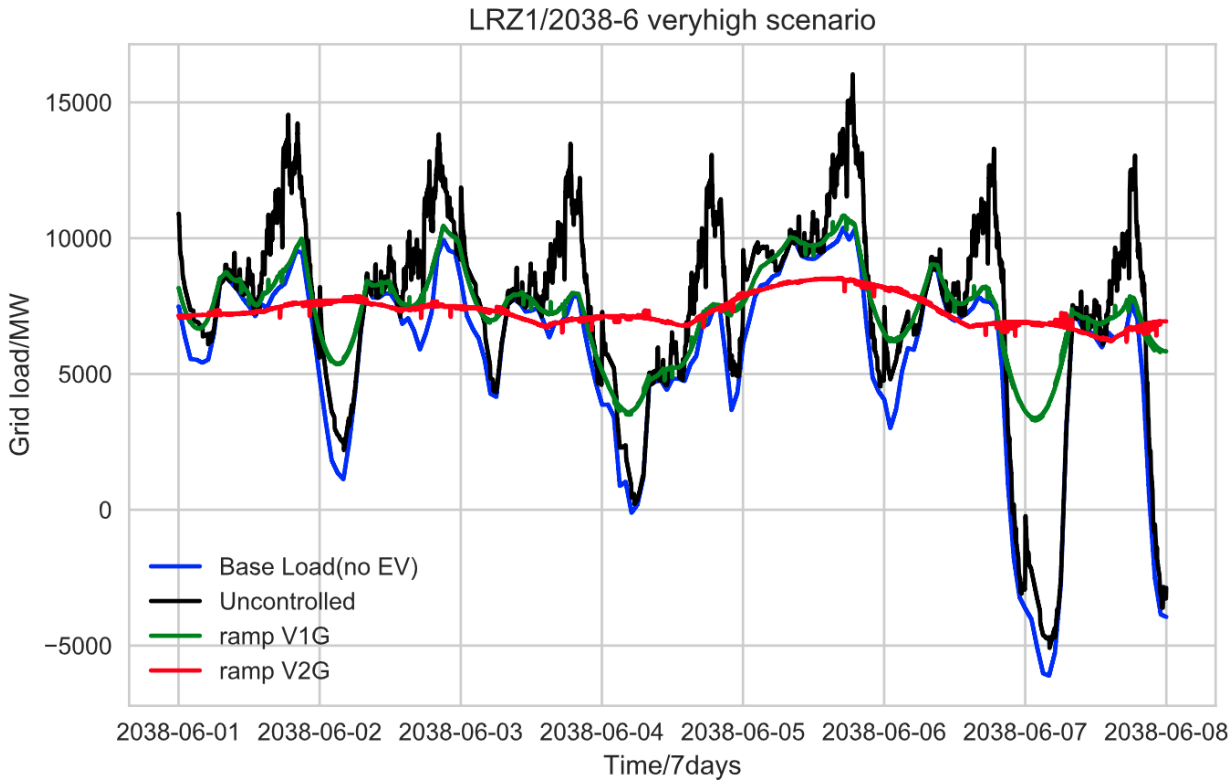

Fig. 31. Very High EV penetration scenario for LRZ 1 in June 2038. Source: Author calculations.

Results for LRZ 7 are shown next. Figs. 32 and 33 show the differences between the Base and Very High EV penetration scenarios, respectively, in June 2033. Note that, unlike the LRZ 1 results, the net load never falls below zero because there is insufficient renewable generation to exceed the gross load. Also unlike in LRZ 1, the Base scenario (Fig. 32) shows more substantial modifications in both the V1G and V2G cases as compared with the uncontrolled charging case, because of the larger proportion of EVs in this LRZ relative to the gross load. In particular, the V2G case (red) is able to greatly reduce the slopes in the load curves, so much so that the time of day at which the deepest part of the valley occurs is shifted earlier by several hours some days (e.g., June 4-7), and the daily peaks are substantially reduced and altered in shape as well.

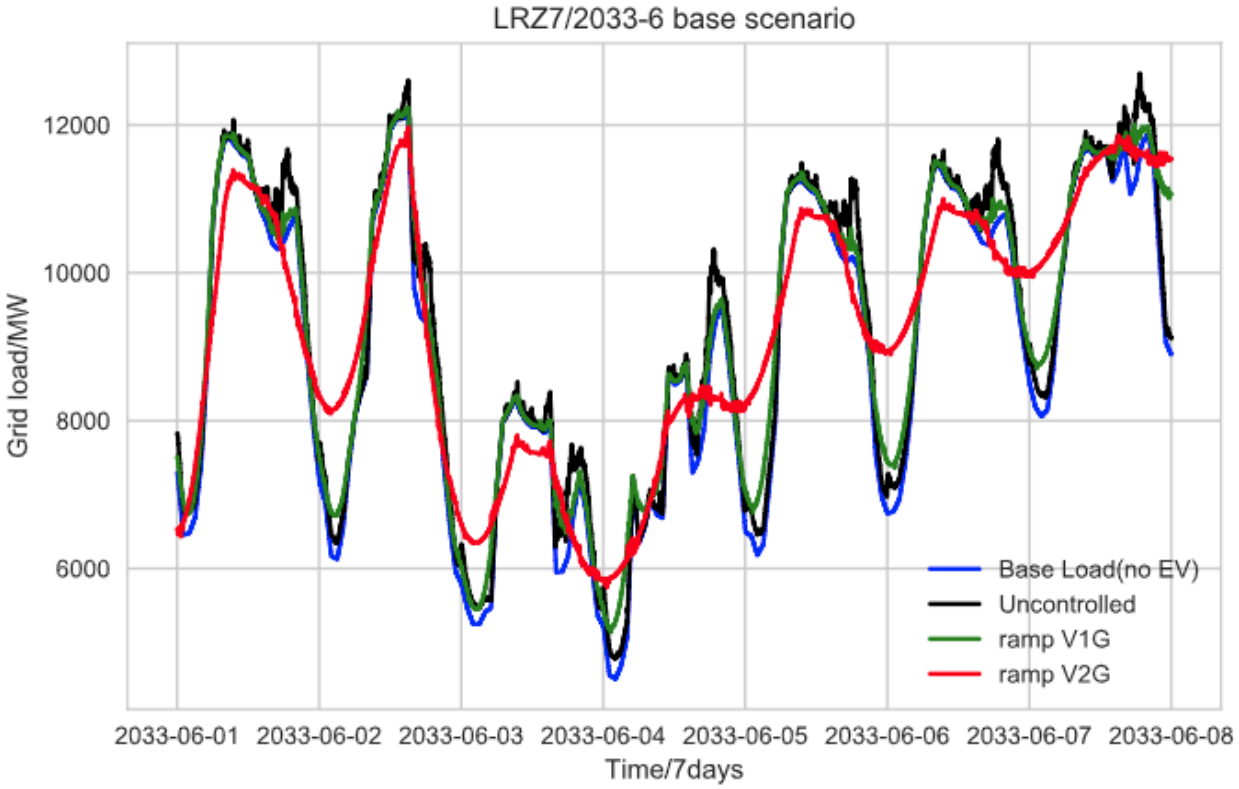

Fig. 32. Base EV penetration scenario for LRZ 7 in June 2033. Source: Author calculations.

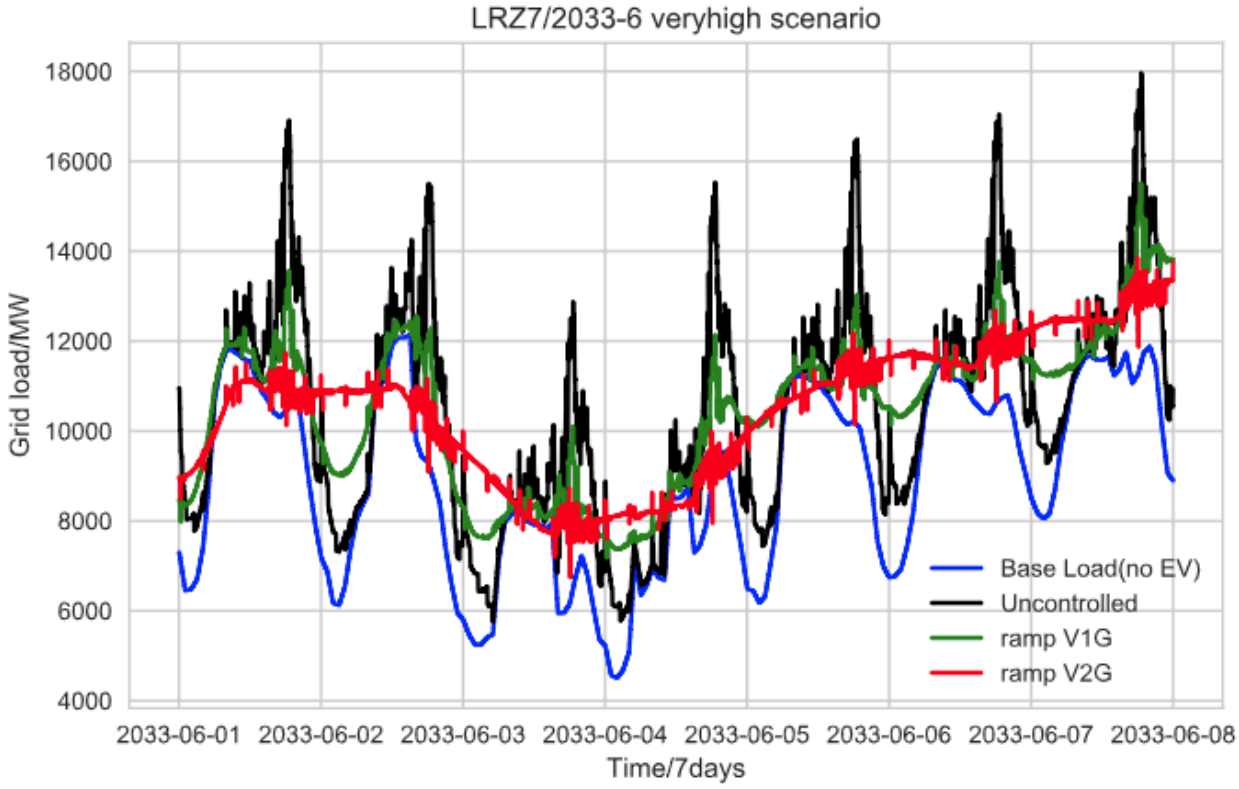

Fig. 33. Very High EV penetration scenario for LRZ 7 in June 2033. Source: Author calculations.

The Very High scenario (Fig. 33) also shows larger amounts of load shaping than in LRZ 1, resulting in a much smoother profile (ignoring spikes that are modeling artifacts) across the week for both the V1G (green) and V2G (red) cases. The V2G case has also become a multi-day optimization.

Figs. 34 and 35 show the same simulations for June 2038. For the Base EV penetration scenario (Fig. 34), there is not much difference in the V1G case (green) other than a deeper filling in of valley loads, but the V2G result (red) again results in much smoother net loads than in the LRZ 1 simulations, with the optimization becoming multi-day.

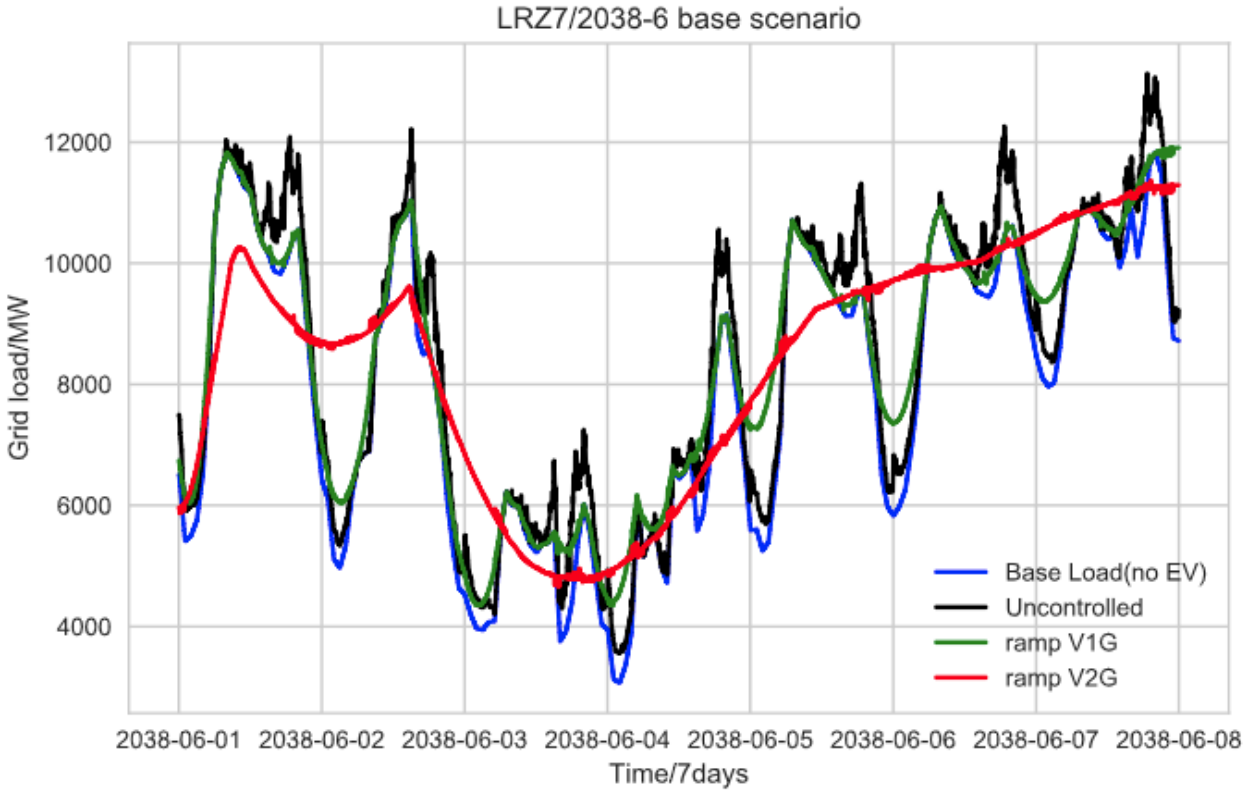

Fig. 34. Base EV penetration scenario for LRZ 7 in June 2038. Source: Author calculations.

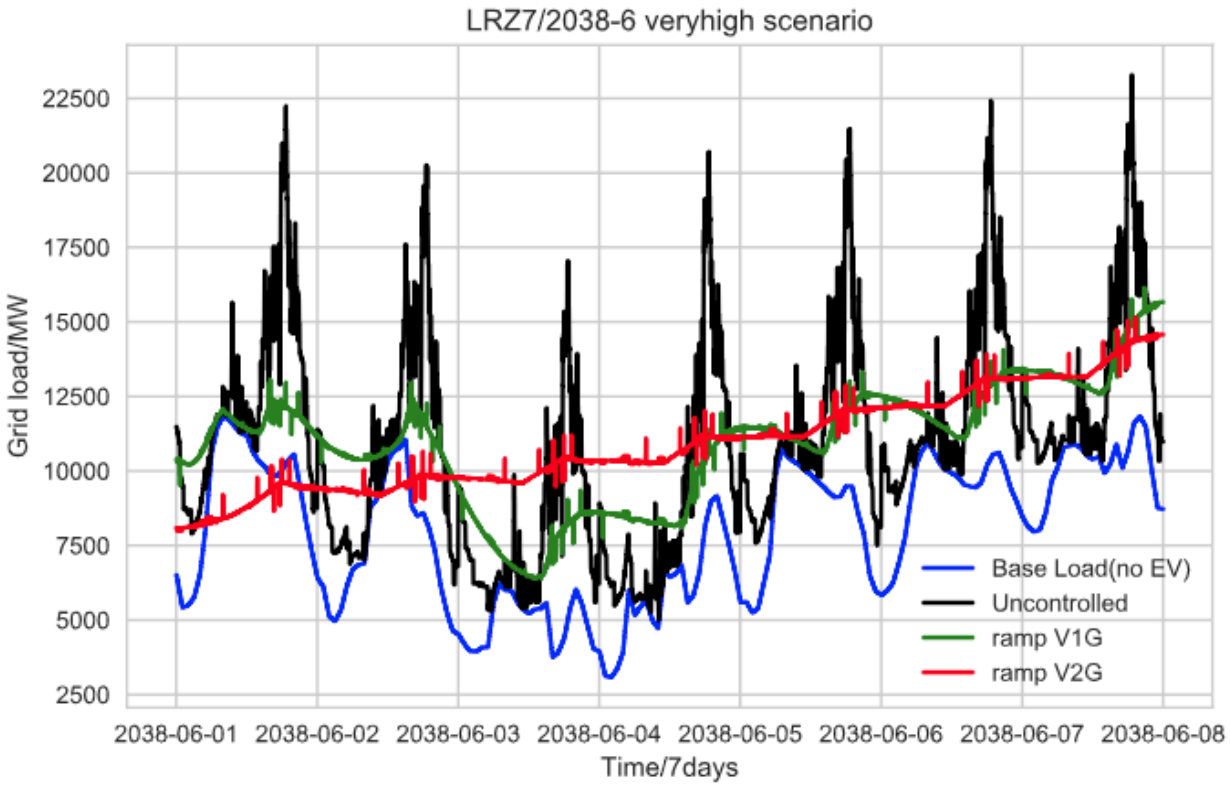

Fig. 35. Very High EV penetration scenario for LRZ 7 in June 2038. Source: Author calculations.

Finally, in the Very High scenario (Fig. 35), while the V1G result (green) has significantly transformed the shape of the load curve, resulting in much lower peaks and shallower valleys, it is still a single-day optimization. By contrast, the V2G result (red) shows very little day-to-day variation, and gently slopes upward over the course of the week, much more so than in Fig. 33.

3.6. Proposed future work

If future funding is provided, we plan to make the following improvements to our analytic approach:

1. Explore peak shaving/ramp mitigation hybrid or other controlled charging protocols as a more optimal algorithm
2. Explore scenarios that blend two or more LRZs
3. Investigate the onset of multi-day optimization as a function of the number of EVs, average vehicle battery size, numbers of charging stations and net load characteristics
4. Improve computational efficiency to allow for more detailed simulations (more intervening years, runs longer than seven days, etc.)
5. Include more EV types in the V2G-Sim model

4. Conclusions

We have performed simulations where variable numbers of EVs are added to the MISO grid as a whole over the 20-year period 2019-2039. Four EV penetration scenarios were performed, ranging from 1.6 to 36 million EVs in 2039. For each penetration scenario, we explored two renewable generation scenarios whose 2039 renewable generation varied by approximately a factor of two: MTEP DET (22%) and RIIA (39%). EVs were allowed to charge in an uncontrolled manner in one scenario, and we explored four types of controlled charging optimizations, consisting of V1G and V2G charging operating under two complementary optimization schemes: peak-valley control, and ramp control. We included a few scenarios where the charging infrastructure assumptions were revised. We also explored optimizations within two local resource zones for the high-renewables (RIIA) scenario: LRZ 1 (consisting primarily of Minnesota, with parts of North Dakota, South Dakota, Wisconsin and Montana) and LRZ 7 (Michigan). These two LRZs were chosen to explore differences in the ratio of renewable generation to the number of EVs.

High-level results indicate that without controlled charging, EVs tend to add load during peak periods of the day, exacerbating generation peaks (P_{max}) and up- and down-ramps ($Ramp_{min}$ and $Ramp_{max}$). In the extreme case of the Very High EV penetration scenario near the end of the simulation period (e.g., in 2038), EV charging dominates loads throughout the day and adds >40,000 MW to peak loads (e.g., see Fig. 21). Fortunately, we also find that all four types of controlled charging optimizations can have an equally profound effect on changing MISO's net load to make it more manageable.

While V1G can be effective at keeping peak daily loads close to what they would be without EVs even at small EV penetrations, by shifting load to other times of day (primarily nighttime load valleys), V2G is able to have a much stronger impact on load shapes for the same numbers of EVs because of its ability to return power to the grid, reducing loads below what they would be without EVS. As a result, V2G optimizations are able to greatly reduce peak loads, and for sufficiently large numbers of EVs, transform daily load variations into profiles that vary slowly over multiple days ("multi-day optimization"). In the extreme case of the Very High EV penetration scenario in 2038, both peak-valley and ramp V2G control optimizations can produce nearly flat loads over the week. But for smaller numbers of EVs, transformations approaching this result are also obtained.

The effect of increasing renewable penetrations on the MISO grid in the absence of EVs is to reduce net loads and exacerbate differences between daily peaks and valleys. These changes lead to somewhat diminished effectiveness of controlled charging on modifying net loads, though the effects are fairly subtle; the conclusion is that while differences in load shape will occur, the controlled charging algorithms are nearly as effective at high renewable penetrations as at lower ones. Critically, controlled charging is able to greatly ameliorate the differences between peaks and valleys caused by renewable generation, producing a net load that is much easier for MISO to manage.

The impact of revising the charging infrastructure assumptions (somewhat less home charging, significantly less workplace charging, and a small increase in the amount of public charging) to

better reflect expected future implementation results in very similar V1G charging profiles, but larger day-to-day load excursions among V2G charging profiles, indicating less load shifting capacity overall. However, the load-shifting capacity is still very significant at a sufficiently high EV penetration level, such as illustrated in the Base EV penetration scenario in 2038 (Fig. 27).

Our exploration of local resource zones indicates that when renewables are sufficiently high as for LRZ 1, net loads can fall below zero, resulting in either an export of excess renewable generation to other LRZs, or renewables curtailment. The effect of the controlled charging algorithms on load shapes is unaffected by the absolute net load level, even when it is negative, and closely resembles results for MISO as a whole. Controlled charging (both V1G and V2G) is able to reduce these negative valleys, and with sufficient numbers of EVs can eliminate them altogether, obviating the need for either export of excess renewable generation or curtailment. For the case where there are more EVs and less renewable generation (e.g., LRZ 7), negative net load does not occur, and the controlled charging algorithms are more effective at shifting loads than for MISO as a whole, due to locally higher numbers of EVs per unit of load.

In conclusion, we have demonstrated that controlled charging can be an effective tool at mitigating both the peak exacerbation effect of large numbers of EVs, as well as increased peak-valley differences (and potentially negative net loads) of high amounts of renewable generation. Whether V1G or V2G, and peak-valley or ramp control, is optimal for MISO will depend on many future assumptions and conditions, and likely a blend of these and other control algorithms will be most suitable to the particular future needs of the MISO grid. However, because of long lead times in deploying and integrating controlled charging equipment with other grid service products, the time is now to start planning for large numbers of EVs on the MISO grid with controlled charging to minimize grid impacts and maximize grid utility.

Acknowledgments

We are indebted to MISO in providing us the opportunity to perform this work, and to Aditya Jayam Prabhakar, John Lawhorn and Ann Benson at MISO, and Wah Sing Ng with NG Planning LLC for their extensive guidance and feedback. We are also grateful to Pamela MacDougall at NRDC for providing key data sources and Jonathan Coignard at Berkeley Lab for coding insight.

References

Alternative Fuels Data Center, no date. Electric Vehicle Infrastructure Projection Tool (EVI-Pro) Lite, Energy Efficiency and Renewable Energy, U.S. Department of Energy. https://afdc.energy.gov/evi-pro-lite. Accessed 21 April 2019.

Amazon, 2019a. OrionMotorTech 110V 16A Portable Electric Car Charger Level 1 for EV EVSE PHEV, 29-1/2ft, UL Recognized Component. https://www.amazon.com/OrionMotorTech-Portable-Electric-Recognized-

Component/dp/B071DM35LT/ref=sr_1_1_sspa?ie=UTF8&qid=1540247654&sr=8-1-spons&keywords=ev+charger+level+1&psc=1. Accessed 23 April 2019.

Amazon, 2019b. Zencar Level 1 EV Charger (110V, 15/16A, 25ft), Portable EVSE Home Electric Vehicle Charging Station Compatible with Chevy Volt, Nissan Leaf, Fiat, Ford Fusion (NEMA 5-15 Plug). https://www.amazon.com/Zencar-Portable-Electric-Charging-Compatible/dp/B077N25YTG/ref=sr_1_3?ie=UTF8&qid=1540247654&sr=8-3&keywords=ev+charger+level+1. Accessed 23 April 2019.

Amazon, 2019c. Morec EV charger Level 2 32 Amp Upgraded Portable Electric Vehicle Charger, NEMA 14-50 220V-240V 26ft (7.9M) EV Charging Cable, SAE J1772 Compatible with All Electric Vehicle Cars. https://www.amazon.com/Morec-Upgraded-Portable-220V-240V-Compatible/dp/B07DHFH8LW/ref=sr_1_1_sspa?ie=UTF8&qid=1540249557&sr=8-1-spons&keywords=ev+charger+level+2&psc=1. Accessed 23 April 2019.

Amazon, 2019d. MUSTART Level 2 Portable EV Charger (240 Volt, 25ft Cable, 40 Amp), Electric Vehicle Charger Plug-in EV Charging Station with NEMA 14-50P. https://www.amazon.com/MUSTART-Portable-Charger-Electric-Charging/dp/B077D5C86M/ref=sr_1_6?ie=UTF8&qid=1540249557&sr=8-6&keywords=ev+charger+level+2&dpID=419EGkiOb2L&preST=_SY300_QL70_&dpSrc=srch. Accessed 23 April 2019.

Amazon, 2019e. Maxgreen EV Charger with Timer, Level 1&2 Electric Vehicle Charger,100-240Volt, 16Amp Electric Car Charger for Timing 2/4/6/8 Hours, Portable EVSE with NEMA 6-20 Plug & NEMA 5-15 Adapter, 25 ft. Cable. https://www.amazon.com/Maxgreen-Electric-100-240Volt-Portable-ft-Cable/dp/B07DWVFLMW/ref=sr_1_fkmr1_3?ie=UTF8&qid=1540252550&sr=8-3-fkmr1&keywords=EV+L1+charger+schedule. Accessed 23 April 2019.

Amazon, 2019f. ChargePoint Home WiFi Enabled Electric Vehicle (EV) Charger - Level 2 240V EVSE, 32A Electric Car Charger for All EVs, UL Listed, ENERGY STAR Certified, Hardwired (no outlet needed), 25 Ft Cable. https://www.amazon.com/ChargePoint-Enabled-Electric-Vehicle-Charger/dp/B071YDGJYZ/ref=sr_1_3?ie=UTF8&qid=1540249557&sr=8-3&keywords=ev+charger+level+2&dpID=51QbxnHlLnL&preST=_SY300_QL70_&dpSrc=srch. Accessed 23 April 2019.

Amazon, 2019g. JuiceBox Pro 40 Smart Electric Vehicle (EV) Charging Station with WiFi - 40 amp Level 2 EVSE, 24-foot cable, NEMA 14-50 plug, UL and Energy Star Certified, Indoor / Outdoor Use. https://www.amazon.com/JuiceBox-Pro-40-JuiceNet-WiFi-equipped/dp/B00UB9R4KO/ref=sr_1_4?ie=UTF8&qid=1540249557&sr=8-4&keywords=ev+charger+level+2&dpID=51lfr6rFmnL&preST=_SY300_QL70_&dpSrc=srch. Accessed 23 April 2019.

Amazon, 2019h. Siemens US2:VC30GRYHW VersiCharge Hard-Wired (VC30GRYHW) : Fast Charging, Easy Installation, Flexible Control, Award Winning, UL Listed, J1772 Compatibility, 14ft Cable, Hard-Wired. https://www.amazon.com/Siemens-US2-VersiCharge-Installation-Compatibility/dp/B00MFVI8UG/ref=sr_1_5?ie=UTF8&qid=1540250481&sr=8-5&keywords=ev+charger+level+2&dpID=31CKNfY5XzL&preST=_SY300_QL70_&dpSrc=srch. Accessed 23 April 2019.

Amazon, 2019i. Siemens VersiCharge Smart-Grid (VCSG30GRYUW): WiFi-equipped, App Controlled, Fast Charging, Easy Installation, Award-Winning, UL Listed, J1772 Compatibility, 20ft Cable, NEMA 6-50 Plug. https://www.amazon.com/dp/B019DKKR7S/ref=emc_b_5_t. Accessed 23 April 2019.

Auto Alliance, 2018. *Advanced Technology Vehicle Sales Dashboard*. https://autoalliance.org/energy-environment/advanced-technology-vehicle-sales-dashboard/. Accessed 14 December 2018.

Auto Alliance, 2019. *Advanced Technology Vehicle Sales Dashboard*. https://autoalliance.org/energy-environment/advanced-technology-vehicle-sales-dashboard/. Accessed 10 April 2019.

Black, D., J. MacDonald, N. DeForest, C. Gehbauer, 2017. *Los Angeles Air Force Base Vehicle-to-Grid Demonstration*, California Energy Commission. Publication Number: CEC-500-2018-025.

Black, D., Y. Rongxin, B. Wang, 2019. *Smart Charging of Electric Vehicles and Driver Engagement for Demand Management and Participation in Electricity Markets*. California Energy Commission. Publication Number: CEC-500-2019-036.

Bloomberg, 2018a. Cumulative Global EV Sales Hit 4 Million, 30 August. https://about.bnef.com/blog/cumulative-global-ev-sales-hit-4-million/. Accessed 10 April 2019.

Bloomberg, 2018b. Electric Vehicle Outlook 2018. https://about.bnef.com/electric-vehicle-outlook/. Accessed 10 April 2019.

Bullard, N., 2019.Electric Car Price Tag Shrinks Along With Battery Cost, *Bloomberg*, April 12. https://www.bloomberg.com/view/articles/2019-04-12/electric-vehicle-battery-shrinks-and-so-does-the-total-cost. Accessed 16 April 2019.

Business Wire, 2018. EDF Energy and Nuvve Corporation Announce Plans to Install 1,500 Smart Electric Chargers in the United Kingdom, 31 October. https://www.businesswire.com/news/home/20181031005476/en/EDF-Energy-Nuvve-Corporation-Announce-Plans-Install. Accessed 16 April 2019.

CAISO, 2019. Demand response - proxy demand resource, California Independent System Operator. http://www.caiso.com/informed/Pages/StakeholderProcesses/CompletedClosedStakeholderInitiatives/DemandResponse-ProxyDemandResource.aspx. Accessed 22 April 2019.

Coignard, J., S. Saxena, J. Greenblatt, D. Wang, 2018. Clean vehicles as an enabler for a clean electricity grid, *Environ. Res. Lett.* 13 054031.

DOE, no date. Renewable Energy Production By State, U.S. Department of Energy. https://www.energy.gov/maps/renewable-energy-production-state. Accessed 16 April 2019.

ElaadNL, 2019. Invade. https://www.elaad.nl/projects/invade/. Accessed 16 April 2019.

EIA, 2018. *Annual Energy Outlook 2018*, Energy Information Administration, U.S. Department of Energy. https://www.eia.gov/outlooks/aeo18/. Accessed 16 April 2019.

EIA, 2019. *Annual Energy Outlook 2019*, Energy Information Administration, U.S. Department of Energy. https://www.eia.gov/outlooks/aeo/. Accessed 16 April 2019.

EVAdoption, 2019. EV Models Currently Available in the US. Last updated 30 March. https://evadoption.com/ev-models/. Accessed 10 April 2019.

Evarts, E. C., 2019. Colorado to launch smart-charging pilot program as it prepares for EVs, *Green Car Reports*, 11 March. https://www.greencarreports.com/news/1121693_colorado-to-launch-smart-charging-pilot-program-as-it-prepares-for-evs. Accessed 16 April 2019.

FleetEurope, 2019. Amsterdam pilots V2G charging, 1 March. https://www.fleeteurope.com/en/smart-mobility/netherlands/article/amsterdam-pilots-v2g-charging?a=FJA05&t%5B0%5D=NewMotion&t%5B1%5D=Alliander&t%5B2%5D=Enervalis&t%5B3%5D=&curl=1. Accessed 16 April 2019.

Fox-Penner, P., W. Gorman, J. Hatch, Long-term U.S. transportation electricity use considering the effect of autonomous-vehicles: Estimates & policy observations, *Energy Policy* 122 (2018) 203–213.

Greenblatt, J. B., 2017. Chapter Three: How will implementation of California's climate policies change the need for underground gas storage in the future? *California Council on Science and Technology,* 1 December. https://ccst.us/wp-content/uploads/Chapter-3-v2.pdf. Accessed 16 April 2019.

Kane, M., 2019. In January Plug-In EV Car Sales In China Almost Tripled: While car sales decreased, plug-ins are conquering the market, *InsideEVs,* 25 February. https://insideevs.com/january-plug-in-car-sales-china-tripled/. Accessed 10 April 2019.

Lipman, T., D. Calloway, 2017. Open Source Platform for Plug-in Electric Vehicle Smart Charging in California (XBOS-V): California Multi-Agency Update on Vehicle-Grid Integration Research, Presentation to the California Energy Commission, 5 December. https://www.energy.ca.gov/research/notices/2017-12-05_workshop/presentations/03_UCB_XBOS-V.pdf. Accessed 22 April 2019.

National Conference of State Legislatures, 2019. State Renewable Portfolio Standards and Goals, 1 February. http://www.ncsl.org/research/energy/renewable-portfolio-standards.aspx. Accessed 16 April 2019.

Newmotion, no date. The Future of EV Charging with V2X Technology. https://newmotion.com/the-future-of-ev-charging-with-v2x-technology. Accessed 16 April 2019.

REN21. 2018. *Renewables 2018 Global Status Report* (Paris: REN21 Secretariat). ISBN 978-3-9818911-3-3. http://www.ren21.net/wp-content/uploads/2018/06/17-8652_GSR2018_FullReport_web_-1.pdf. Accessed 16 April 2019.

Slowik, P., N. Lutsey, 2018. *The continued transition to electric vehicles in U.S. cities*, International Council on Clean Transportation white paper, July.

Smart Energy International, 2019. The UK pilots smart EV charging hubs with V2G and storage, 27 March. https://www.smart-energy.com/industry-sectors/electric-vehicles/the-uk-pilots-smart-ev-charging-hubs-with-v2g-and-storage/. Accessed 16 April 2019.

Veloz, 2019. Detailed Sales Chart, 5 April. http://www.veloz.org/wp-content/uploads/2019/04/3_mar_2019_Dashboard_PEV_Sales_veloz.pdf. Accessed 10 April 2019.

Wang, D., J. Coignard, T. Zeng, C. Zhang, S. Saxena, 2016. Quantifying electric vehicle battery degradation from driving vs. vehicle-to-grid services, *Journal of Power Sources* 332: 193-203. https://doi.org/10.1016/j.jpowsour.2016.09.116.

Wikipedia, 2019. Phase-out of fossil fuel vehicles, Last updated 27 March. https://en.wikipedia.org/wiki/Phase-out_of_fossil_fuel_vehicles. Accessed 10 April 2019.

World Population Review, no date. US States - Ranked by Population 2018. http://worldpopulationreview.com/states/. Accessed 21 April 2019.

Contact information

Jeffery Greenblatt, jeff@emerging-futures.com, +1 (510) 693-6452
Cong Zhang, congzhang@lbl.gov, +1 (323) 686-1128
Samveg Saxena, ssaxena@lbl.gov, +1 (510) 269-7260